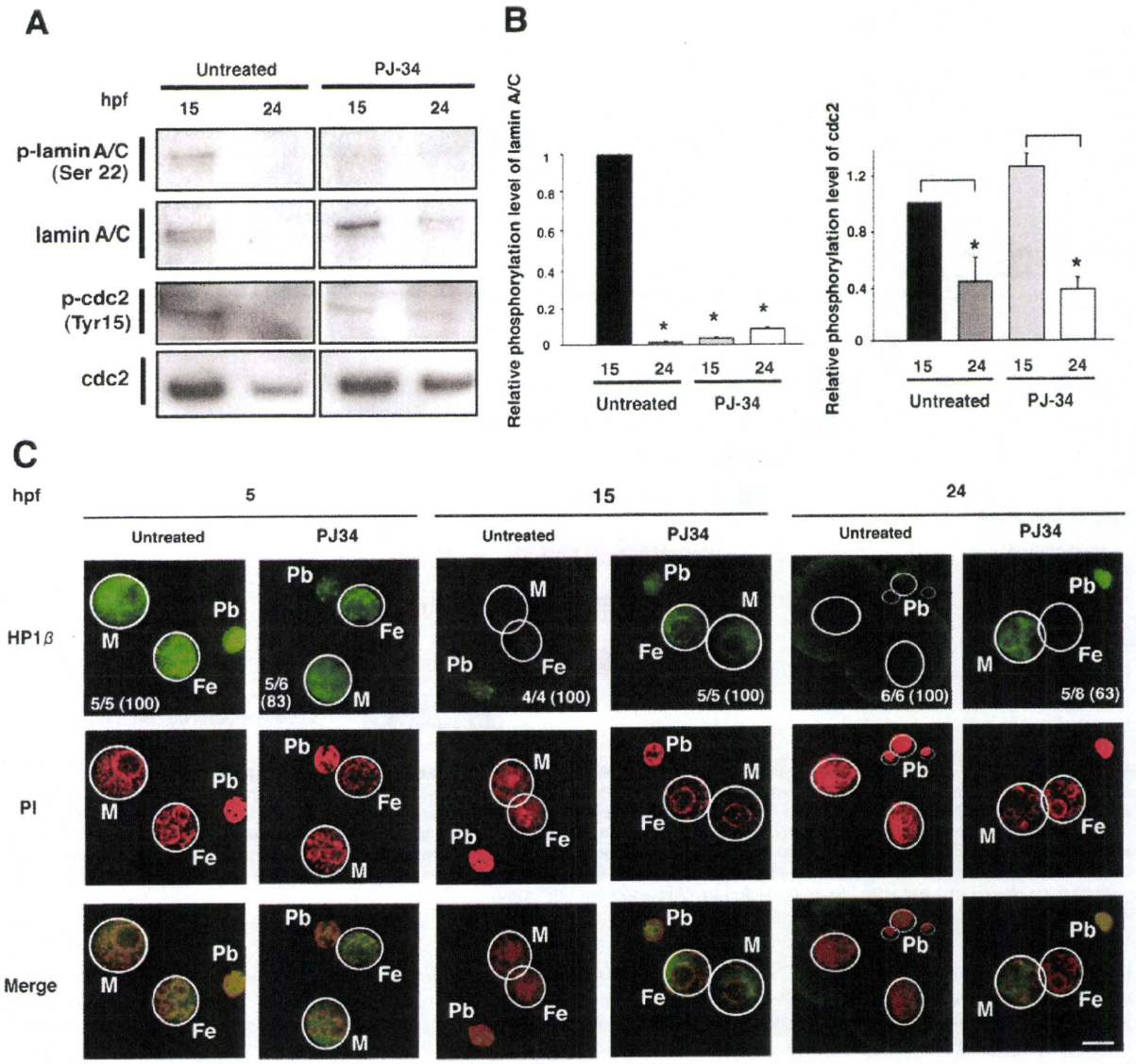

Figure 6. Defective phosphorylation of pronuclear lamins and behavior of HP1β during postfertilization development. Extracts from 100 untreated or PARylation inhibited embryos at 15 and 24 hpf were immunoblotted with antibody for phosphorylated lamin A/C, total lamin A/C, phosphorylated cdc-2, and total cdc-2 (**A**). Assessments for the relative phosphorylation levels of lamin and cdc2. Asterisks represent statistic significance (t test, $p<0.05$) (**B**). Immunofluorescence with laser-scanning confocal microscopy of untreated and PJ-34 treated embryos with antibodies for HP1β (**C**). Detected antigens were colored with green. DNA counterstained with PI was colored in red. Colocalized signals of antigens and DNA were colored in orange or yellow in merged figures. Circles (white lines) show the outlines of the female (Fe) and male (M) PNs. Other PI signals represent polar bodies (Pb). Values (percentage in parenthesis) represent frequency of the staining in each panel (**C**, upper panels). Bar represents 25 μm.
doi:10.1371/journal.pone.0012526.g006

embryos (Figure 6C). HP1ß was still detectable only in male PNs of one cell embryos by PARylation inhibition, but undetectable at the nuclei of two-cell embryos in 24 hpf embryos in the absence of PJ-34 treatment (Figure 6C). This data implies that PJ-34 delayed the HP1ß removal from chromatin of PNs and this could be involved in attenuated phosphorylation of lamin A/C.

Discussion

Our data from studies by pharmacological inhibition of PARylation in mice suggests that PARylation has three major functions in peri-fertilization processes (Figure 7). First, PARylation affects proper spindle formation in the mouse MII oocytes. Our data supports the view of Parp function described in a previous study using *Xenopus* oocytes [31]. The a/ß-tubulins, which have been reported as major components of microtubules, are shown to be acceptor proteins for PARylation in mouse oocytes [32]. Our data suggest that PARylation may regulate the meiotic spindle assembly of MII oocytes either directly through PTM of tubulin, indirectly by altering MAPK signaling, or both. Immunofluorescence study showed no specific localization of PAR signals in MII-oocytes, while spindle bundle formation is

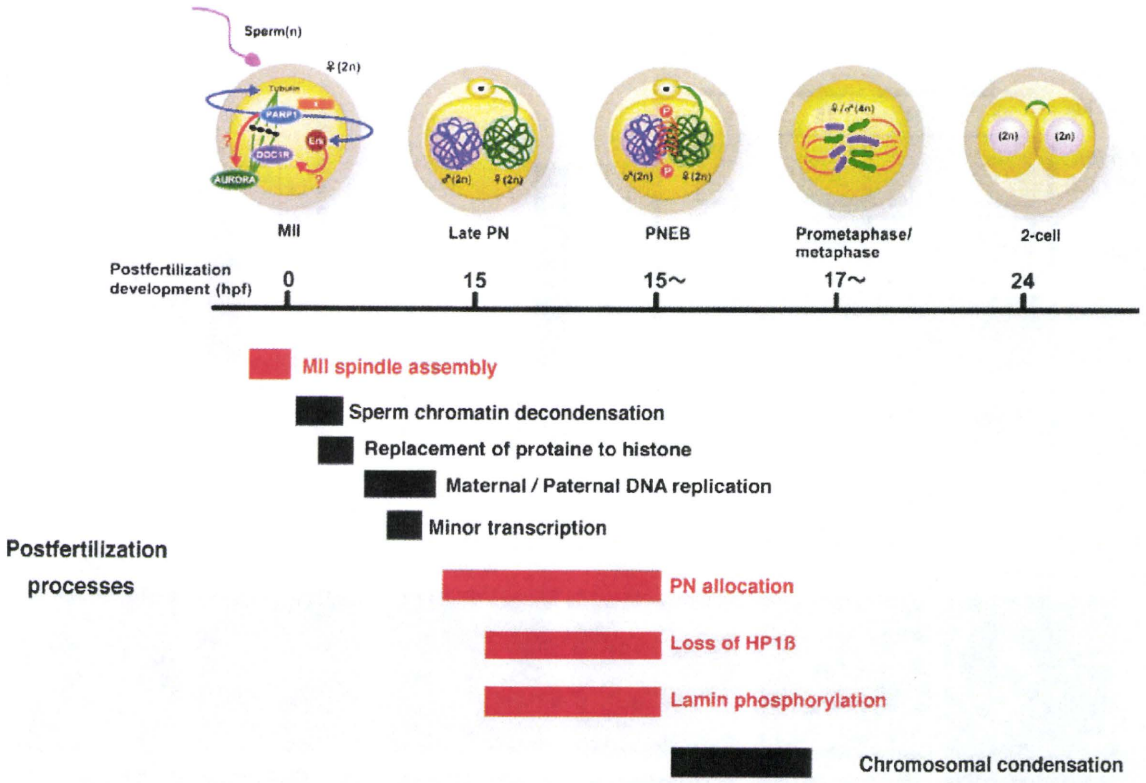

Figure 7. Scheme of spacio-temporal regulation by PARylation during perifertilization mouse development. At MII oocytes, Parp1 or other Parps are involved in spindle bundle formation mediated in part by Erk phosphorylation, which is represented as MII spindle assembly. Other Parp-associated molecules (Aurora [47]) or MAPK-associated molecules such as DOC1R [48] putatively contribute to spindle formation integrity. HP1ß loss from PNs and PN allocation are interfered by Parp inhibitors during PN stages. Phosphorylation of lamin A/C is reduced by PARylation inhibition, and subsequently PNEB is blocked. Because HP1β is associated with both chromatin and nuclear envelope, both chromatin and nuclear envelope are putatively regulated by PARylation. Duration of biological processes during 24 hrs after fertilization (open square) is listed temporally and those marked in red have been suggested to be regulated by PARylation from this study.
doi:10.1371/journal.pone.0012526.g007

perturbed by PARylation inhibition. Cytoplasmic tubulins are broadly present in mouse oocytes and associated with Erk and kinesins. Cytoplasmic Parp1 is associated with microtubule mediated by kinesins and modulates Erk signaling in neurons [24,25,33]. Our data shows downregulation of phosphorylation of Erk-1/2 in *Parp1*$^{-/-}$ MII oocytes. Collectively, we speculate that Parp1 may act as an activator of Erk-1/2 phosphorylation in the MII oocytes. Spindle bundle formation could be also regulated by other tubulin-associated Parps (Figure 6). Related to this view, interaction of tankyrase-1 with NuMA as an acceptor protein of poly(ADP-ribose) was reported to regulate mitotic spindle assembly [34]. Phosphorylation of Erks is downregulated in *Parp1*$^{-/-}$ eggs before and after activation. However, it seems that a low level of Parp1-independent phosphorylation of Erk is induced after activation, although Erk signaling is gradually inactivated upon fertilization in normal development. The PAR signals induced on meiotic spindles for a brief period during postfertilization development suggest that spindle-associated Parp1 is activated, that could mediate the Erk-signaling upon fertilization.

Intracytoplasmic Ca^{2+} release stimulates the NAD metabolism after binding of sperm to the egg cell membrane [35]. Parp catalyzes PARylation of proteins using NAD with production of nicotinamide. Thus, we speculate a novel possibility that PARylation functions as a mediator of NAD signals upon fertilization.

Second, the inhibition of PARylation results in the complete inhibition of PNEB. Mechanism of PNEB remains largely unknown. The phosphorylation of nuclear lamins is a major process in PNEB. Here, we showed that the phosphorylation of lamins A and C is hampered by the inhibition of PARylation. Interestingly, although the cdc2 kinase activity is responsible for the phosphorylation of the lamin meshwork, our data indicates that these activities are intact in PJ-34-treated embryos. Lamin A negatively affects epigenetic regulation of the myogenin gene expression in mouse myoblasts [36]. Synthesis of lamin A is absent during the cleavage-stage blastomere [37] and in stem cells [38]. Recently, Parp1 was found to co-localize with HP1 that promotes the interaction of heterochromatin with the inner layer of the nuclear envelope [29]. We found that, in contrast to untreated embryos, HP1ß signals were persistently detected in the male PNs of PJ-34-treated embryos at 24 hpf. Together with the evidence from a previous study describing that PARylation also functions in telomere regulation [39], our data raise the possibility that PARylation functions as a regulatory machinery of the pronuclear envelope disassembly.

Our data using PJ-34 and 5-AIQ was different from those obtained with 3-aminobenzamide (3-AB) [22]. We found that IVF

experiments and *in vitro* culture of one-cell embryos with 5 mM 3-AB did not show any influence on the transition of the first mitotic cleavage. In this study, we did not observe the inhibition of PAR activation at the PN stage by 5 mM 3-AB (data not shown). Our immunofluorescence showed residual signals of PAR at the PNs of embryos treated with 5 mM 3-AB, but barely with PJ-34 and 5-AIQ. Collectively, we found that PJ-34 or 5-AIQ, water-soluble PARP inhibitors, are more suitable for a more precise assessment of inhibition of total PARylation activity at postfertilization development. Further analyses will be needed to seek for the functional PARPs, which regulate MII spindle assembly, signal transduction of PNEB processes during early stages of postfertilization development.

Recently, PARylation inhibitors emerge as effective therapeutic agents for mammary tumors [40]. Our study also implicates a risk of subfertility by administrating PARP inhibitors. Furthermore this study raises a possibility of PARP inhibitors as potent contraceptive chemicals. Molecular dissection of the PARylation system will provide our understanding for significance of PTM in mammalian development [41].

Materials and Methods

Oocyte and embryo manipulations

Parp1$^{-/-}$ mutant mice under a B6D2F1 hybrid background were generated by sequential backcrosses of *Parp1*$^{+/-}$ mice to C57BL/6J and DBA2/J [11]. Oocytes were collected from superovulated B6D2F1 females 14 hrs after the intraperitoneal injection of equine chorionic gonadotropin (eCG), followed by the injection of human chorionic gonadotropin (hCG). For IVF, oocytes were cultured in TYH medium [42]. Sperm was collected from the caudal epididymis of B6D2F1 males and incubated in TYH medium. After the preincubation of MII oocytes in 200/300 μL of TYH medium with or without PJ-34 or 5-AIQ as described in Table 1, sperm (150 sperm/μL) was added to the oocytes. Intracytoplasmic sperm injection (ICSI) was carried out essentially as described previously [43]. ICSI was carried out in Hepes-buffered CZB medium with or without 30 μM PJ-34. Thereafter, embryos were cultured in modified Whitten medium [44].

Animal care

All animals were housed according to the institutional guidelines in compliance with National Institutes of Health guidelines. Experiments using animals were approved by the Animal Care and Use committee of Mitsubishi Kagaku Institute of Life Sciences, MITILS, and National Cancer Center Research Institute (T05-026-MB06, T05-026-CB07).

Antibodies

The antibodies and dilutions used in this study were described in Supplemental Table S1. The HRP–conjugated rat or rabbit IgG (1:10000, Jackson Immunoresearch Laboratory) and HRP-conjugated mouse IgG (1:1000, Bio-Rad) as the secondary antibodies for immunodetection and the Alex Fluor conjugates (1:200, Invitrogen) of IgG for immunofluorescence.

Immunofluorescence

The cumulus-oocyte complex was dissociated by hyaluronidase (Sigma) and the zona pellucida was removed with 0.5% actinase (Kaken, Japan). After incubation of the denuded oocytes or embryos for at least 30 minutes, the oocytes or embryos were placed into fibrin clots [45]. The fibrin clots were prepared by mixing 1 μl fibrinogen (12.5 mg/ml PBS: Calbiochem) with 1 μl thrombin (10 mg/ml distilled H_2O: Sigma). For the staining of microtubules, oocytes and embryos were permeabilized by microtubule stabilizing buffer (60 mM PIPES, 25 mM HEPES, 10 mM EGTA, 2 mM $MgCl_2$, adjusted to pH 6.9) for 3 minutes, and then fixed with 3% formaldehyde for 10 minutes at 37°C. The cells were incubated with primary antibodies for 1 hr or overnight at 37°C, followed by incubation with blocking buffer (PBS containing 5% normal goat serum and 0.05% Tween-20). The cells were then incubated with secondary antibodies for 1–2 hrs at 37°C. After washing with PBS, the cells were counterstained with PI and subjected to microscopic analyses. For the staining with histone modification antibodies, the cells were fixed with 4% paraformaldehyde for 15 minutes at 4°C and then permeabilized with PBS containing 0.1% BSA and 0.5% TritonX-100 for 10 minutes. The cells were incubated with primary antibodies overnight at 4°C, and then with secondary antibodies for at least 3 hrs at 4°C. For detection of DNA synthesis, the IVF embryos at 8 hpf were transferred to Whitten medium containing 10 μM 5-bromo-2′-deoxyuridine (BrdU, Roche Diagnostic Corporation) and incubated for 2 hrs. Embryos were then fixed and permeabilized as described above. After washing for three times, embryos were incubated in culture medium containing 2 N HCl for 30 min. Embryos were washed for 5 times with borate buffer (pH 8.5) and then for 3 times with PBS. Neutralized embryos were incubated for 30 min with PBS containing 5% FBS, and then reacted with anti-bromodeoxyuridine monoclonal antibody (Roche Diagnostic Corporation) overnight at 4°C. The images were captured under a light microscopy (Axiophot, Zeiss) or confocal microscopy (IX71 with Fluoview FV300, Olympus) system.

Immunoblots

For the two-dimensional gel electrophoresis, oocyte extracts were collected into sample buffer (7 M urea, 2 M thio-urea, 4% CHAPS, 40 mM DTT, 2% IPG buffer (pH 3–10) (GE Healthcare), protease inhibitor cocktail). Samples were purified using the 2D Clean-UP kit (GE Healthcare). Protein extracts corresponding to 300 MII oocytes or one-cell embryos were applied to an Immobiline drystrip (pH 3–10, GE Healthcare) and subjected to isoelectric focusing with a multiphor apparatus (GE Healthcare) as the first protein separation. The stripe was then applied to a 10% SDS-PAGE gel for the second protein separation. The proteins on the gels were transferred to a BioTrace nitrocellulose membrane for histones WB (pore size, 0.2 μm, Pall) or Immobilon PVDF membrane (Millipore), and reacted with primary antibodies for 1 hr at room temperature. The membrane was washed and then reacted with secondary HRP-conjugated antibodies (see below). The signals were enhanced by Can Get Signal, an immunoreaction enhancer solution (Toyobo) and detected with the Chemi-Lumi One kit (Nacalai) and Amersham Hyperfine ECL (GE Healthcare).

Parg analysis

Eggs in the Parg buffer (20 mM potassium phosphate (pH 7.5), 0.1% Triton X-100, 10 mM §-mercaptoethanol) were mixed for 30 minutes at 4°C by a mixer, and then subjected to freezing and thawing five times. Aliquots of the extracts corresponding to 2 eggs were used for the thin layer chromatography (TLC) assay. Fifteen nanograms of recombinant GST-Parg (0.3 μL) were used as control. Extracts were incubated for 2 hrs at 25°C with ^{32}P-labeled PAR. The reactions were terminated by adding 0.1% SDS. The samples were spotted on a polyethylene impregnated cellulose TLC plate (Macherht-Nagal), developed with a developing buffer [46], and then detected by BAS2500 (Fuji Film).

RT-PCR

Total RNA was isolated from 100–150 MII oocytes using Sepasol-RNA I Super (Nacalai). The cDNA was synthesized by Superscript III (Invitrogen) according to the manufacturer's instructions. The PCR reactions were carried out at 55 and 60°C as the annealing temperature with 30 and 40 cycles. The primer sequences used in this study and expected length of amplified cDNA fragments were described in Table S2.

Supporting Information

Table S1 The primary antibodies used in this study.
Found at: doi:10.1371/journal.pone.0012526.s001 (0.13 MB TIF)

Table S2 The primer sequences to detect *Parps*, *Parg*, and *G3pdh* genes by RT-PCR.

Found at: doi:10.1371/journal.pone.0012526.s002 (9.44 MB TIF)

Acknowledgments

We thank Dr. I. Kitabayashi, Dr. T. Jenuwein, and Dr. T. Takeuchi for providing antibodies and plasmids, and Dr. T. Sugimura, Dr. R. Yanagimachi, Dr. K. Yanagida, and Dr. K. Naito for their informative insights and suggestions, and Miss R. Umeda, and Miss K. Oda for technical assistance.

Author Contributions

Conceived and designed the experiments: TO MM. Performed the experiments: TO HO TH SI AO. Analyzed the data: TO HO MM. Contributed reagents/materials/analysis tools: TH KN AO TN MM. Wrote the paper: TO MM.

References

1. Yanagimachi R (1994) Mammalian fertilization. In: Knobil E, Neil JD, eds. Physiology of Reproduction. 2nd edition. New York: Raven Press. pp 189–317.
2. Florman H, Ducibella T (2007) Mammalian fertilization. In: Neil JD, P.M. Wassarman PM, eds. Knobil and Neill's Physiology of Reproduction. 3rd edition. Amsterdam, Netherlands: Elsevirer. pp 55–112.
3. Rawe VY, Olmedo SB, Nodar FN, Ponzio R, Sutovsky P (2003) Abnormal assembly of annulate lamellae and nuclear pore complex coincides with fertilization arrest at the pronuclear stage of human zygotic development. Hum Reprod 18: 576–582.
4. Telford NA, Watson AJ, Schultz GA (1990) Transition from maternal to embryonic control in early mammalian development: a comparison of several species. Mol Reprod Dev 26: 90–100.
5. Fan HY, Sun QY (2004) Involvement of mitogen-activated protein kinase cascade during oocyte maturation and fertilization in mammals. Biol Reprod 70: 535–547.
6. Vignon X, Zhou Q, Renard JP (2002) Chromatin as a regulative architecture of the early developmental functions of mammalian embryos after fertilization or nuclear transfer. Cloning Stem Cells 4: 363–377.
7. Santos F, Peters AH, Otte AP, Reik W, Dean W (2005) Dynamic chromatin modifications characterize the first cell cycle in mouse embryos. Dev Biol 280: 225–236.
8. Schultz RM (1993) Regulation of zygotic gene activation in the mouse. Bioassay 15: 531–538.
9. Sugimura T, Miwa M (1994) Poly(ADP-ribose): historical perspective. Mol Cell Biochem 138: 5–12.
10. Schreiber V, Dantzer F, Ame JC, de Murcia G (2006) Poly(ADP-ribose): novel functions for an old molecule. Nat Rev Mol Cell Biol 7: 517–528.
11. Masutani M, Suzuki H, Kamada N, Watanabe M, Ueda O, et al. (1999) Poly(ADP-ribose) polymerase gene disruption conferred mice resistant to streptpzptpcin-induced diabetes. Proc Natl Acad Sci U S A 96: 2301–2304.
12. Menissier de Murcia J, Ricoul M, Tartier L, Niedergang C, Huber A, et al. (2003) Functional interaction between PARP-1 and PARP-2 in chromosome stability and embryonic development in mouse. EMBO J 22: 2255–2263.
13. Koh DW, Lawler AM, Poitras MF, Sasaki M, Wattler S, et al. (2004) Failure to degrade poly(ADP-ribose) causes increased sensitivity to cytotoxicity and early embryonic lethality. Proc Natl Acad Sci U S A 101: 17699–17704.
14. Abdelkarim GE, Gertz KK, Harms C, Katchanov J, Dirnagl U, et al. (2001) Protective effects of PJ-34, a novel, potent inhibitor of poly(ADP-ribose) polymerase (PARP) *in vitro* and *in vivo* models of stroke. Int J Mol Med 7: 255.
15. McDonald MC, Mota-Filipe H, Wright JA, Abdelrahman M, Threadgill MD, et al. (2000) Effects of 5-aminoisoquinolinone, a water-soluble, potent inhibitor of the activity of poly(ADP-ribose) polymerase on the organ injury and dysfunction caused by hemorrhagic shock. Br J Pharmacol 130: 843–850.
16. Erdelyi K, Kiss A, Bakondi E, Bai P, Szabo C, et al. (2005) Gallotannin inhibits the expression of chemokines and ainflammatory cytokines in A549 cells. Mol Pharmacol 68: 895–904.
17. Huang D, Yang C, Wang Y, Liao Y, Huang K (2009) PARP-1 suppresses adiponectin express9oin through poly(ADP-ribosyl)ation of PPAR gamma in cardiac fibroblasts. Cardiovasc Res 81: 98–107.
18. Bakondi E, Bai P, Szabo EE, Hunyadi J, Gergely P, et al. (2002) Detection of poly(ADP-ribose) polymerases activation in oxidatively stressed cells and tissues using biotinylated NAD substrate. J Histochem Cytochem 50: 91–98.
19. Valdor R, Schreiber V, Saenz L, Martinez T, Munoz-Suano A, et al. (2008) Regulation of NFAT by poly(ADP-ribose) polymerase activity in T cells. Mol Immunol 45: 1863–1871.
20. Fossati S, Cipriani G, Moroni F, Chiarugi A (2007) Neither energy collapse nor transcription underlie in vitro neurotoxicity of poly(ADP-ribose) polymerase hyper-activation. Neurochem Int 50: 203–210.
21. Inbar-Rozensal D, Castiel A, Visochek L, Castel D, Dantzer F, et al. (2009) A selective eradication of human nonhereditary breast cancer cells by phenanthridine-derived polyADP-ribose polymerase inhibitors. Breast Cancer Res 11: R78.
22. Imamura T, Neildez TM, Thenevin C, Paldi A (2004) Essential role for poly(ADP-ribosyl)ation in mouse preimplantation development. BMC Mol Biol 5: 4.
23. Tong C, Fan HY, Chen DY, Song XF, Schatten H, et al. (2003) Effects of MEK inhibitor U0126 on meiotic progression in mouse oocytes: microtubule organization, asymmetric division and metaphase II arrest. Cell Res 13: 375–383.
24. Kauppinen TM, Chan WY, Suh SW, Wiggins AK, Huang EJ, et al. (2006) Direct phosphorylation and regulation of poly(ADP-ribose) polymerase-1 by extracellular signal-regulated kinases 1/2. Proc Natl Acad Sci USA 103: 7136–7141.
25. Cohen-Armon M, Visochek L, Roensal D, Kalal A, Geistrikh I, et al. (2007) DNA-independent PARP-1 activation by phosphorylated ERK2 increases Elk1 activity: a link to histone acetylation. Mol Cell 26: 297–308.
26. Gerace L, Blobel G (1980) The nuclear envelope lamina is reversibly depolymerized during mitosis. Cell 19: 277–287.
27. Schatten G, Maul GG, Schatten H, Chaly N, Simerly C, et al. (1985) Nuclear lamins and peripheral nuclear antigens during fertilization and embryogenesis in mice and sea urchins. Proc Natl Acad Sci U S A 82: 4727–4731.
28. Peter M, Nakagawa J, Doree M, Labbe JC, Nigg EA (1990) *In vitro* disassembly of the nuclear lamina and M phase-specific phosphorylation of lamins by cdc2 kinase. Cell 61: 591–602.
29. Quenet D, Gasser V, Fouillen L, Cammas F, Sanglier-Cianferani S, et al. (2008) The histone subcode: poly(ADP-ribose) polymerase-1 (Parp-1) and Parp-2 control cell differentiation by regulating the transfcriptional intermediary factor TIF beta and heterochromatin protein HP1alpha. FASEB J 22: 3853–3865.
30. Arney KL, Bao S, Bannister AJ, Kouzarides T, Surani MA (2002) Histone methylation defines epigenetic asymmetry in the mouse zygotes. Int J Dev Biol 46: 317–320.
31. Chang P, Jacobson MK, Mitchison TJ (2004) Poly(ADP-ribose) is required for spindle assembly and structure. Nature 432: 645–649.
32. Satchell MA, Zhang X, Kochanek PM, Dixon CE, Jenkins L, et al. (2003) A dual role for poly-ADP-ribosylation in spatial memory acquisition after traumatic brain injury in mice. J Neuroses 83: 697–708.
33. Midorikawa R, Takei Y, Hirokawa N (2006) KIF4 motor regulates activity-dependent neuronal survival by suppressing PARP-1 enzymatic activity. Cell 125: 371–383.
34. Chang P, Coughlin M, Mitchison TJ (2009) Interaction between Poly(ADP-ribose) and NuMA contributes to mitotic spindle pole assembly. Mol Biol Cell 20: 4575–4585.
35. Epel D, Patton C, Wallace RW, Cheung WY (1981) Calmodulin activates NAD kinase of sea urchin eggs: an early event of fertilization. Cell 23: 543–549.
36. Hakelien AM, Delbarre E, Kristine G, Gaustad KG, Berndia B, et al. (2008) Expression of the myodystrophic R453W mutation of lamin A in C2C12 myoblasts causes promoter-specific and global epigenetic defects. Exp Cell Res 314: 1869–1880.
37. Clarke HJ (1992) Nuclear and chromatin composition of mammalian gametes and early embryos. Biochem Cell Biol 70: 856–866.
38. Pajerowski JD, Dahl KN, Zhong FL, Sammak PJ, Discher DE (2007) Physical plasticity of the nucleus in stem cell differentiation. Porc Natl Acad Sci USA 104: 15619–15624.
39. Smith S, Giriat I, Schmitt A, de Lange T (1998) Tankylase, a poly(ADP-ribose) polymerase at human telomere. Science 282: 1484–1487.
40. Fong PC, Boss DS, Yap TA, Tutt A, Wu P, et al. (2009) Inhibition of poly(ADP-ribose) polymerase in tumor from BRCA mutation carriers. N Engl J Med 361: 123–134.
41. Sims RJ, 3rd, Reinberg D (2008) Is there a code embedded in proteins that is based on post-translational modifications? Nat Rev Mol Cell Biol 9: 815–820.

42. Toyoda Y, Yokoyama M, Hoshi T (1971) Studies on the fertilization of mouse eggs in vitro. J Anim Reprod 16: 147–151.
43. Osada T, Toyoda A, Moisyadi S, Akutsu H, Hattori M, et al. (2005) Production of inbred and hybrid transgenic mice carrying lathe (>200 kb) foreign DNA fragments by intracytoplasmic sperm injection. Mol Reprod Dev 72: 329–335.
44. Whitten WK, Biggers JD (1968) Complete development in vitro of the pre-implantation stages of the mouse in a simple chemically defined medium. J Rrprod Fertil 17: 399–401.
45. Simerly C, Schatten G (1993) Techniques for localization of specific molecules in oocytes and embryos. Methods Enzymol 225: 516–553.
46. Shimokawa T, Masutani M, Nagasawa S, Nozaki T, Ikota N, et al. (1999) Isolation and cloning of rat poly(ADP-ribose) glycohydrolase: presence of a potential nuclear export signal conserved in mammalian orthologs. J Biochem 126: 748–755.
47. Monaco L, Kolthur-Seetharam U, Loury R, Murcia JM, de Murcia G, et al. (2005) Inhibition of Aurora-B-kinase activity by poly(ADP-ribosyl)ation in response to DNA damage. Proc Natl Acad Sci U S A 102: 14244–14248.
48. Terret ME, Lefebvre C, Djiane A, Rassinier P, Moreau J, et al. (2003) DOC1R: a MAP kinase substrate that control microtubule organization of metaphase II mouse oocytes. Development 130: 5169–5177.

Role of Poly(ADP-ribosylation) Reaction in Response to Ionizing Radiation

イオン化放射線への応答におけるポリADP-リボシル化反応の役割

Hidenori Shirai[1], Takashisa Hirai[1,2], Erika Sasamoto[1], Aki Inase[1], Hideki Ogino[1], Keisuke Sasai[2], Takashi Sugimura[1], Mitsuko Masutani[1]

1) Biochemistry Division, National Cancer Center Research Institute
2) Department of Radiology School of Medicine, Juntendo University

白井 秀徳[1]、平井 崇久[1,2]、笹本 絵里香[1]、稲瀬 安希[1]
荻野 秀樹[1]、笹井 啓資[2]、杉村 隆[1]、益谷 美都子[1]*
1)国立がん研究センター　研究所　生化学部
2)順天堂大学　医学部　放射線医学講座

(*mmasutan@ncc.go.jp)

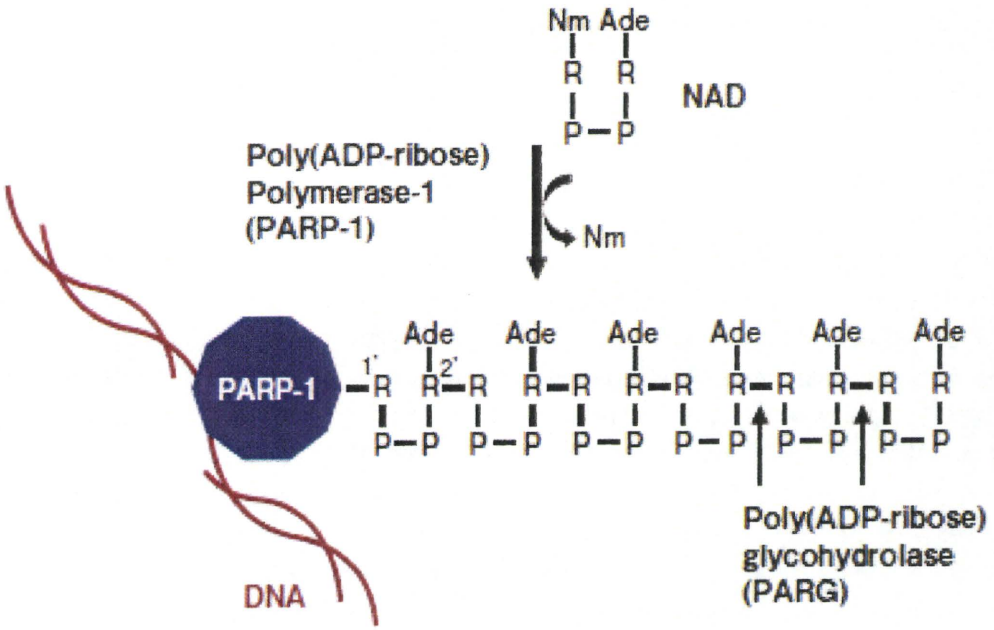

Fig. 1. PolyADP-ribosylation reaction. Ade, adenine; R, ribose; P, phosphate; Nm, nicotinamide.
図1：ポリADP-リボシル化反応。Ade＝アデニン；R＝リボース；P＝リン酸；Nm＝ニコチンアミド。

Poly(ADP-ribose) polymerase (PARP) catalyzes the poly(ADP-ribosylation) reaction using β-NAD^+as a substrate (Figs. 1 and 2). Sixteen members of PARP family proteins are now known. *Parp-1*$^{-/-}$ ES cells and mice show increased lethality against γ-irradiation and alkylating agents. After γ-irradiation, *Parp-1*$^{-/-}$ mice showed more severe villous atrophy of the small

ポリ（ADP-リボース）合成酵素（PARP）は、β-NAD^+を基質としてポリADP-リボシル化反応を触媒する（図1、2）。PARPファミリーの蛋白質は、現在16種類が知られている。*Parp-1*$^{-/-}$ ES細胞とマウスは、γ線照射とアルキル化剤処理に対して野生型より放死感受性が亢進している。γ線照射実験では、*Parp-1*$^{-/-}$マウスは、*Parp-1*$^{+/+}$マウスに比して重度の小腸絨毛萎縮を呈した。胸腺での髄外造血の

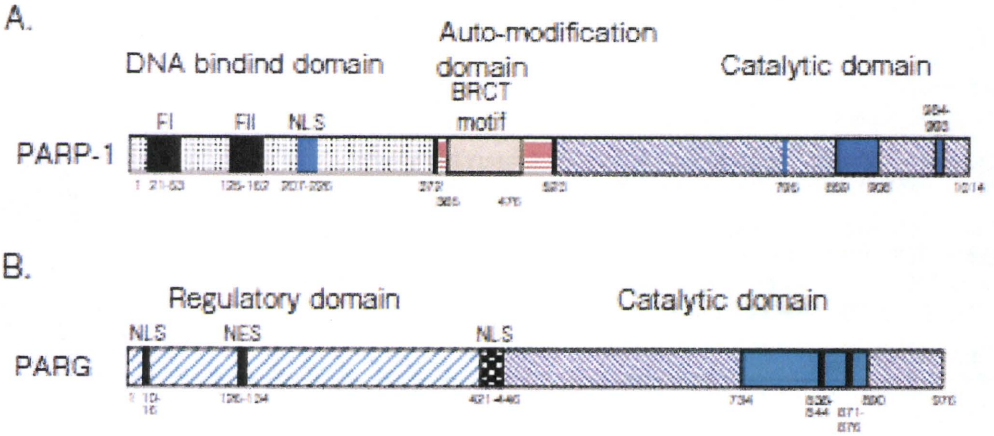

Fig. 2. Domain structure of human PARP-1 and PARG. A, PARP-1; B, PARG. The numbers indicate amino acid residues.
図2：ヒトPARP-1およびPARGのドメイン構造。A, PARP-1；B, PARG。数値はアミノ酸残基数を示す。

intestine compared to *Parp-1*$^{+/+}$ mice. A defect in extramedullary hematopoiesis in the spleen was observed, accompanying hemorrhage in the tissues, such as glandular stomach and testes (Fig. 3). *Parp-1*$^{+/+}$ mice show increased frequencies of point-mutation and deletion-type mutation after γ-irradiation. In contrast, *Parp-1*$^{-/-}$ mice showed no increase in the frequency of deletion-type mutation, whereas the frequency of point-mutation was increased as in *Parp-1*$^{+/+}$ mice. Deletion-type mutations are mainly caused by inaccurate repair through non-homologous end-joining (NHEJ). The result thus suggests that *Parp-1* deficiency blocks NHEJ repair after γ-irradiation, which leads to deletion mutation.

Poly(ADP-ribose) is mainly degraded by poly(ADP-ribose) glycohydrolase (PARG) into ADP-ribose (Figs.1 and 2). *Parg*$^{-/-}$ mouse ES cells showed increased lethality against treatment with an alkylating agent and cisplatin. Sensitization to γ-irradiation was observed in *Parg*$^{-/-}$ mouse ES cells. Therefore, inhibition of PARG may be useful for sensitization to radiation therapy.

欠損が見られ、腺胃や精巣などの組織での出血を伴っていた（図3）。*Parp-1*$^{+/+}$ マウスでは、γ線照射後に点突然変異と欠失型突然変異の頻度が上昇した。対照的に *Parp-1*$^{-/-}$ マウスでは、欠失型突然変異の頻度は上昇せず、点突然変異の頻度は *Parp-1*$^{+/+}$ マウスと同様に増加した。欠失型突然変異は、主として非相同末端結合（NHEJ）による不正確な修復によって引き起こされる。本研究の結果は、γ線照射後、欠失型突然変異を誘導するNHEJ修復が *Parp-1* を欠損することにより阻害されるため、欠失型突然変異が誘発されないことを示唆している。

ポリ（ADP-リボース）は、主としてポリ（ADP-リボース）グリコヒドロラーゼ（PARG）によって分解され、ADP-リボースになる（図1、2）。*Parg*$^{-/-}$ マウスES細胞は、アルキル化剤とシスプラチン処理に対する致死感受性が増加した。*Parg*$^{-/-}$ マウスES細胞では、γ線照射への致死感受性の亢進が見られた。したがって、PARGの阻害は放射線治療の増感に有用であると考えられる。

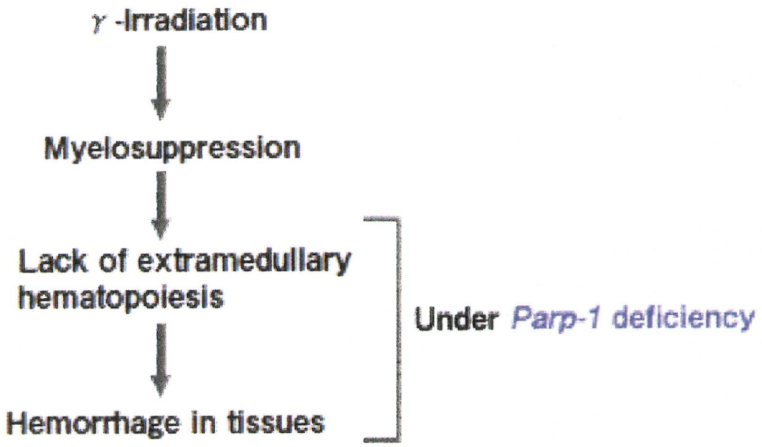

Fig. 3. A model for hemorrhage in tissues of *Parp-1*$^{-/-}$ mice after γ-irradiation.
図3：γ線照射後の*Parp-1*$^{-/-}$マウスにおける組織内出血のモデル。

References

1. Fujihara H, Masutani M, *et al. Poly(ADP-ribose) glycohydrolase* deficiency sensitizes mouse ES cells to DNA damaging agents. Curr. Cancer Drug Targets, 2009, 9:953-962.
2. Shibata A, Masutani M, *et al.* Role of Parp-1 in suppressing spontaneous deletion mutation in the liver and brain of mice at adolescence and advanced age. Mutation Res., 2009, 664:20-27.
3. Shibata A, Masutani M, *et al. Parp-1* deficiency causes an increase of deletion mutations and insertions/rearrangements *in vivo* after treatment with an alkylating agent. Oncogene, 2005, 24:1328-1337.
4. Masutani, M, *et al*. The response of Parp knockout mice against DNA damaging agents. Mutation Res., 2000, 462:159-166.
5. Nozaki, T, Masutani, M, *et al*. Suppression of G1 arrest and enhancement of G2 arrest by inhibitors of poly(ADP-ribose) polymerase: possible involvement of poly(ADP-ribosyl)ation in cell cycle arrest following γ -irradiation. Jpn. J. Cancer Res., 1994, 85:1094-1098.

THE JOURNAL OF BIOLOGICAL CHEMISTRY VOL. 285, NO. 23, pp. 17442–17452, June 4, 2010

Secretory Mechanisms and Intercellular Transfer of MicroRNAs in Living Cells*[S]◆

Received for publication, January 26, 2010, and in revised form, March 8, 2010 Published, JBC Papers in Press, March 30, 2010, DOI 10.1074/jbc.M110.107821

Nobuyoshi Kosaka[‡1], Haruhisa Iguchi[‡§1], Yusuke Yoshioka[‡], Fumitaka Takeshita[‡], Yasushi Matsuki[§], and Takahiro Ochiya[‡2]

From the [‡]Section for Studies on Metastasis, National Cancer Center Research Institute, 5-1-1, Tsukiji, Chuo-ku, Tokyo 104-0045 and the [§]Pharmacology Research Laboratories, Dainippon Sumitomo Pharma Company, Limited, 1-98, Kasugadenaka 3-chome, Konohana-ku, Osaka 554-0022, Japan

The existence of circulating microRNAs (miRNAs) in the blood of cancer patients has raised the possibility that miRNAs may serve as a novel diagnostic marker. However, the secretory mechanism and biological function of extracellular miRNAs remain unclear. Here, we show that miRNAs are released through a ceramide-dependent secretory machinery and that the secretory miRNAs are transferable and functional in the recipient cells. Ceramide, whose biosynthesis is regulated by neutral sphingomyelinase 2 (nSMase2), triggers secretion of small membrane vesicles called exosomes. The decreased activity of nSMase2 with a chemical inhibitor, GW4869, and a specific small interfering RNA resulted in the reduced secretion of miRNAs. Complementarily, overexpression of nSMase2 increased extracellular amounts of miRNAs. We also revealed that the endosomal sorting complex required for transport system is unnecessary for the release of miRNAs. Furthermore, a tumor-suppressive miRNA secreted via this pathway was transported between cells and exerted gene silencing in the recipient cells, thereby leading to cell growth inhibition. Our findings shed a ray of light on the physiological relevance of secretory miRNAs.

It has been well known that extracellular RNAs circulate in the blood of healthy people and diseased patients with sufficient integrity, although ribonuclease is present in both plasma and serum (1). The spectrum of RNAs whose presence was demonstrated in plasma and other body fluids, such as urine and breast milk, extends from housekeeping genes to fetal genes detected in pregnant women and genes overexpressed in a variety of different tumors (2). To explain the stability of circulating RNAs, it was suggested that extracellular RNAs are included within lipoprotein vesicles. Indeed, exogenous RNAs added to plasma or blood are immediately degraded, whereas endogenous plasma RNAs are stable for hours under the same conditions (3). Moreover, the treatment of some detergents results in immediate degradation of plasma extracellular RNAs, apparently due to disruption of the lipid vesicles. These findings clearly indicate that extracellular RNAs are packaged in some kinds of secretory particles including apoptotic bodies and exosomes, and thus, they are protected from dominantly existing ribonucleases.

Apoptotic bodies are small membranous particles released during programmed cell death (4), and exosomes are small intraluminal vesicles (50–100 nm in diameter) of multivesicular bodies (MVB)[3] released on exocytic fusion of MVB with plasma membranes (5). Currently, accumulating evidence suggests that these secretory vesicles can function as intercellular transmitters to convey their contents, in particular, microRNA (miRNA) (6–8). Recent studies reported that extracellular exosomal miRNAs were transferred into other cells and that apoptotic bodies delivered miR-126 into endothelial cells (9). Despite these advances, however, the underlying mechanism of the secretory process and the biological function of circulating miRNAs are not yet fully understood.

miRNAs, small 20–22-nucleotide-long members of the non-protein-coding RNA family, are expressed in the vast majority of eukaryotes, including humans (10). Not only do they inhibit translation of their target genes, they also degrade the target mRNAs through recognition of imperfect complementary sites, usually located in the 3′-untranslated regions of the target mRNAs, endowing miRNAs with the capacity to regulate numerous biological processes. Over the past several years, it was evident that dysregulations of many kinds of miRNAs have been linked to the initiation and progression of human cancer (11). Interestingly, the amounts of secretory miRNAs are up-regulated in the plasma of patients bearing tumors, including B cell lymphoma, prostate cancer, lung cancer, and ovarian cancer (12–15). Thus, detection and monitoring of tumors are now becoming possible by the evaluation of tumor-derived secretory miRNAs.

In this study, we have shown that secretion of miRNAs is controlled by neutral sphingomyelinase 2 (nSMase2), which is known as a rate-limiting enzyme of ceramide biosynthesis. Fur-

* This work was supported in part by a grant-in-aid for the third-term comprehensive 10-year strategy for cancer control, a grant-in-aid for scientific research on priority areas cancer from the Ministry of Education, Culture, Sports, Science and Technology, and the Program for Promotion of Fundamental Studies in Health Sciences of the National Institute of Biomedical Innovation (NiBio).

◆ This article was selected as a Paper of the Week.

[S] The on-line version of this article (available at http://www.jbc.org) contains supplemental Figs. 1–5.

[1] Both authors contributed equally to this work.

[2] To whom correspondence should be addressed: Section for Studies on Metastasis, National Cancer Center Research Institute, 1-1, Tsukiji, 5-chome, Chuo-ku, Tokyo 104-0045, Japan. Tel.: 81-3-3542-2511, Ext. 4800; Fax: 81-3-3541-2685; E-mail: tochiya@ncc.go.jp.

[3] The abbreviations used are: MVB, multivesicular bodies; Alix, ALG-2 interacting protein; ESCRT, endosomal sorting complex required for transport; miRNA, microRNA; nSMase2, neutral sphingomyelinase 2; siRNA, small interfering RNA; QRT-PCR, quantitative real time PCR; CM, conditioned medium.

thermore, we provide evidences that miRNAs secreted from donor cells can be taken up and function in the recipient cells. These findings propose a novel mechanism of intercellular communication mediated by secretory miRNAs.

EXPERIMENTAL PROCEDURES

Reagents—Rabbit polyclonal anti-nSMase2 (H-195) (sc-67305), goat polyclonal anti-Alix (Q-19) (sc-49268), and donkey anti-goat IgG (horseradish peroxidase) (sc-2020) were purchased from Santa Cruz Biotechnology. Rabbit polyclonal anti-ROCK1 (ab36746) was from Abcam. Mouse monoclonal anti-actin, clone C4 (MAB1501), was from Millipore. Anti-CD63 monoclonal antibody was purchased from BD Pharmingen. Peroxidase-labeled anti-mouse and anti-rabbit antibodies were included in the Amersham Biosciences ECL PLUS Western blotting reagents pack (RPN2124) (GE HealthCare). Synthetic *Caenorhabditis elegans* miRNA cel-miR-39 was synthesized by Qiagen (Valencia, CA). Synthetic hsa-miR-146a (pre-miR-146a) was purchased from Ambion (Austin, TX). The duplexes of each small interfering RNA (siRNA), targeting human nSMase2 mRNA (s30925; target sequences of 5′-GGAGGUGUUUGACAAGCGAdTdT-3′ and 5′-UCGCUUGUCAAACACCUCCtg-3′), and negative control 1 (NC1) were purchased from Applied Biosystems, and an siRNA specific for human ALG-2 interacting protein (Alix) mRNA (target sequences of 5′-GAACCUGGAUAAUGAUGAAdTdT-3′ and 5′-UUCAUCAUUAUCCAGGUUCdTdT-3′) was purchased from Sigma-Genosys. GW4869 was purchased from Calbiochem (Darmstadt, Germany). Cisplatin was obtained from Alexis (Lausen, Switzerland). Geneticin was purchased from Invitrogen.

Cell Culture—HEK293 cells, a human embryonic kidney cell line (CRL-1573), and COS-7 cells, an African green monkey kidney fibroblast-like cell line (CRL-1651), were obtained from the American Type Culture Collection (Manassas, VA). These cells were cultured in Dulbecco's modified Eagle's medium containing 10% heat-inactivated fetal bovine serum and antibiotic-antimycotic (Invitrogen) at 37 °C in 5% CO_2. PC-3M-luc cells (Xenogen) were cultured in RPMI containing 10% heat-inactivated fetal bovine serum and antibiotic-antimycotic at 37 °C in 5% CO_2.

Preparation of Conditioned Medium and Exosome—Prior to collection of culture medium, HEK293 and COS-7 cells were washed three times with Advanced RPMI containing antibiotic-antimycotic and 2 mM L-glutamine (medium A), and the medium was switched to fresh medium A. After incubation during 3 days, medium A was collected and centrifuged at 2,000 × *g* for 15 min at room temperature. To thoroughly remove cellular debris, the supernatant was centrifuged again at 12,000 × *g* for 35 min at room temperature. Then the conditioned medium was used for miRNA extraction and functional assays as well as exosome isolation.

For exosome preparation, the conditioned medium was ultracentrifuged at 110,000 × *g* for 70 min at 4 °C. The pellets were washed with 11 ml of phosphate-buffered saline, and after ultracentrifugation, they were resuspended in phosphate-buffered saline. The exosome fraction was measured for its protein content using the Micro BCA protein assay kit (Thermo Scientific).

Isolation of MicroRNAs—Isolation of extracellular and cellular miRNAs was performed using the mirVana isolation kit (Ambion). One hundred μl of conditioned medium or cell lysate was diluted with 200 μl of lysis/binding solution. After a 5-min incubation, 20 μl of miRNA homogenate additive and 1 μl of 1 nM cel-miR-39 were added to each aliquot, followed by vortex for 30 s and incubation on ice for 10 min. Subsequent phenol extraction and filter cartridge work were carried out according to the manufacturer's protocol.

RNA Detection—Detection of RNAs was performed by using the Agilent Bioanalyzer 2100 (Agilent Technologies). Prior to the analysis, total RNAs were prepared with the Agilent RNA 6000 Pico kit (Agilent Technologies) according to the manufacturer's protocol.

RNase Treatment—To evaluate whether small RNAs were present inside the exosomes, RNase mixture (Ambion) was added to conditioned medium at a final concentration of 5 units/ml RNase A and 200 units/ml RNase T1 and then incubated at 37 °C for 30 min. Small RNAs were purified using the mirVana miRNA isolation kit (Ambion) as described above.

Quantitative Real Time PCR (QRT-PCR)—The method for QRT-PCR has been previously described (13). PCR was carried out in 96-well plates using the 7300 Real Time PCR System (Applied Biosystems). All reactions were done in triplicate. All of the TaqMan microRNA assays were purchased from Applied Biosystems. cel-miR-39 and hRNU6 were used as invariant control for conditioned medium and cell, respectively. The concentrations of extracellular miRNAs were calculated based on their C_t values normalized by those of cel-miR-39, which was spiked in each aliquot of QRT-PCR reaction at 1 nM.

Immunoprecipitation—Conditioned medium was incubated with magnetic beads (Invitrogen) coated with purified anti-CD63 antibody or mouse IgG1 control antibody (Millipore) at 4 °C overnight. After washing with phosphate-buffered saline, miRNAs were extracted and applied to QRT-PCR.

Immunoblot Analysis—SDS-PAGE gels (SuperSep Ace 5–20%, 194-15021, Wako) were calibrated with Precision Plus protein standards (161-0375) (Bio-Rad), and anti-CD63 (1:100), anti-nSMase2 (1:200), anti-Alix (1:100), anti-ROCK1 (1:200), and anti-actin (1:1,000) were used as primary antibodies. The dilution ratio of each antibody is indicated in parentheses. Two secondary antibodies (peroxidase-labeled anti-mouse and anti-rabbit antibodies) were each used at a dilution of 1:10,000. Bound antibodies were visualized by chemiluminescence using the ECL Plus Western blotting detection system (RPN2132) (GE HealthCare), and luminescent images were analyzed by a LuminoImager (LAS-3000; Fuji Film Inc.).

Plasmids—psiRNA-LucGL3 was purchased from InvivoGen. Primary-miR-143 and primary-miR-146a expression vectors were purchased from TaKaRa BIO. A full-length human nSMase2 cDNA was cloned into pIRES2-EGFP vector (Clontech). Primary miRNAs (pri-miR-155, pri-miR-16, and pri-miR-21) were PCR-amplified from human genomic DNA and cloned into the downstream of cytomegalovirus promoter in pIRES2-EGFP. For luciferase-based reporter gene assays, pLuc-Neo was constructed by inserting a firefly luciferase gene

derived from pGL3-control (Promega) into pEYFP-1 vector (Clontech) at the BglII and AflII sites. Sensor vector for miR-146a was constructed by introducing tandem binding sites with perfect complementarity to miR-146a, separated by a four-nucleotide spacer into the NotI site of psiCHECK2 (Promega). The sequences of the binding site are as follows: 5′-AAACCTAGAGCGGCCGCAACCCATGGAATTC***AGTTCTCA***AAGAATTCTTAACCCATGGAATTC***AGTTCTCA***GCGGCCGCTGGCCGCAA-3′ (sense) and 5′-TTGCGGCCAGCGGCCGCTGAGAACTGAATTCCATGGGTTAAGAATTCTTTGAGAACTGAATTCCATGGGTTGCGGCCGCTCTAGGTTT-3′ (antisense). The "seed" sequence of miR-146a is indicated in bold and italics. In a mutated miR-146a sensor vector, the seed sequence, AGTTCTCA, was displaced with CTGGAGAC. All the plasmids were verified by DNA sequencing.

Transient Transfection Assays—Plasmid transfections to HEK293 and COS-7 cells were performed using Lipofectamine LTX (Invitrogen). Cell numbers and amounts of plasmids for each transfection were determined according to the manufacturer's protocol.

Transfections of siRNA and miRNA were accomplished with DharmaFECT transfection reagent (Thermo Scientific) according to the manufacturer's protocol. The total amounts of small RNAs for each transfection were equally adjusted by the addition of NC1.

Establishment of Stable Cell Lines—Stable HEK293 cell lines expressing firefly luciferase or miR-146a were generated by selection with 300 μg/ml Geneticin. HEK293 cells were transfected with 0.5 μg of pLucNeo vector or pri-miR-146a expression vector at 90% confluency in 24-well dishes using a Lipofectamine LTX reagent in accordance with the manufacturer's instructions. Twelve h after the transfection, the cells were replated in a 10-cm dish followed by a 3-week selection with the antibiotic. Ten surviving single colonies were picked up from each transfectant and were then cultured for another 2 weeks. The cells expressing the largest amount of firefly luciferase or miR-146a among transfectants were used as luciferase stably expressing cells and miR-146a stably expressing cells, respectively.

Luciferase Reporter Assay—HEK293 and COS-7 cells were cultured at a density of 5×10^4 and 1×10^4 cells/well, respectively, in 96-well tissue culture plates overnight, and miRNA transfections or the addition of conditioned medium were performed as described under the legend for Figs. 5–7. The cells were harvested, and *Renilla* luciferase activity was measured and normalized by firefly luciferase activity(16). All assays were performed in triplicate and repeated at least three times, and the most representative results are shown.

Cell Growth Assay—PC-3M-luc cells were seeded at a density of 2×10^3 cells/well in a 96-well plate. The following day, the cells were transfected with mature miRNAs or were incubated with a conditioned medium. Twenty-four h later, the culture medium of the transfected cells was switched to medium A, whereas the conditioned medium was not changed. After a 3-day culture, cells were harvested for the measurement of firefly luciferase activity.

Measurement of Caspase-3/7 Activities—On day 0, HEK293 cells were seeded at a density of 2.5×10^4 cells/well in a 96-well tissue culture plate. The following day, the cells were transfected with nSMase2 expression vector or were treated with 10 μM cisplatin. On day 2, the cells were applied to an Apo-ONE homogeneous caspase-3/7 assay (Promega). After a 12-h incubation, the fluorescence of each well was measured at an excitation wavelength of 480 nm and an emission wavelength of 520 nm using Envision (Wallac).

RESULTS

Overexpression of miRNA in Cells Leads to an Increased Secretion—To reveal the physiological roles of extracellular miRNAs, we investigated the mechanism of their secretion and whether or not secretory miRNAs can function in cells beyond their own cell origin. Based on the observation that expression patterns of miRNAs in a cell and culture medium are well correlated (7, 17), we hypothesized that up-regulation of cellular miRNAs leads to an increase of extracellular miRNAs in a conditioned medium. To test this hypothesis, we quantified the amount of extracellular and cellular miRNAs (miR-16, -21, -143, -146a, and -155) in HEK293 and COS-7 cells transfected with each primary miRNA expression vector or empty vector. We avoided the use of synthetic analogues of mature miRNAs for this overexpression experiment because they might persist in the medium and interfere with accurate quantification of extracellular miRNAs. The transfected cells were thoroughly washed prior to the medium change to remove any surplus liposome left by the original transfection. QRT-PCR analysis showed that secretion of the miRNAs was enhanced in proportion to their cellular amounts induced by the transfections of pri-miRNA vectors (Fig. 1*A*; supplemental Fig. 1*A*). To exactly estimate what percentages of the miRNAs were excreted, we re-evaluated cellular amounts of the miRNAs by the same normalization method as the extracellular miRNAs (supplemental Fig. 1*B*). As a result of the calculations, the amounts of secreted miRNAs were quite lower in conditioned medium than in parental cells. The ratios of secreted miRNAs/cellular miRNAs are shown as follows: endogenous miR-16, 1.21 ± 0.12%; endogenous miR-21, 1.62 ± 0.63%; exogenous miR-143, 2.57 ± 1.03%; exogenous miR-146a, 15.6 ± 1.62%; exogenous miR-155, 1.38 ± 0.84%. Additionally, siRNAs targeting luciferase were also released from the siRNA-overexpressing cells (Fig. 1*B*). We further observed that endogenous miR-16 and -21 as well as overexpressed miR-146a time-dependently accumulated in the conditioned medium during 96 h (Fig. 1*C*). We observed by microscopic examination that these cells did not suffer from any damage and that they maintained the original cell shape. Moreover, the treatment of an apoptotic inducer, cisplatin, did not increase the miRNA secretion (data not shown). These findings strongly suggest that living cells can actively secrete endogenous and exogenous miRNAs as well as artificial small RNAs.

Secreted miRNAs Are Contained in Exosomes—It was revealed that exosomes can transfer some of their contents to other cell types, and importantly, that miRNAs exist in exosomes and are protected from RNases (6). First, we isolated exosome fractions from HEK293 cells by the standard ultracen-

Supplemental Material can be found at:
http://www.jbc.org/content/suppl/2010/03/30/M110.107821.DC1.html
http://www.jbc.org/content/suppl/2010/05/28/285.23.17442.DC1.html

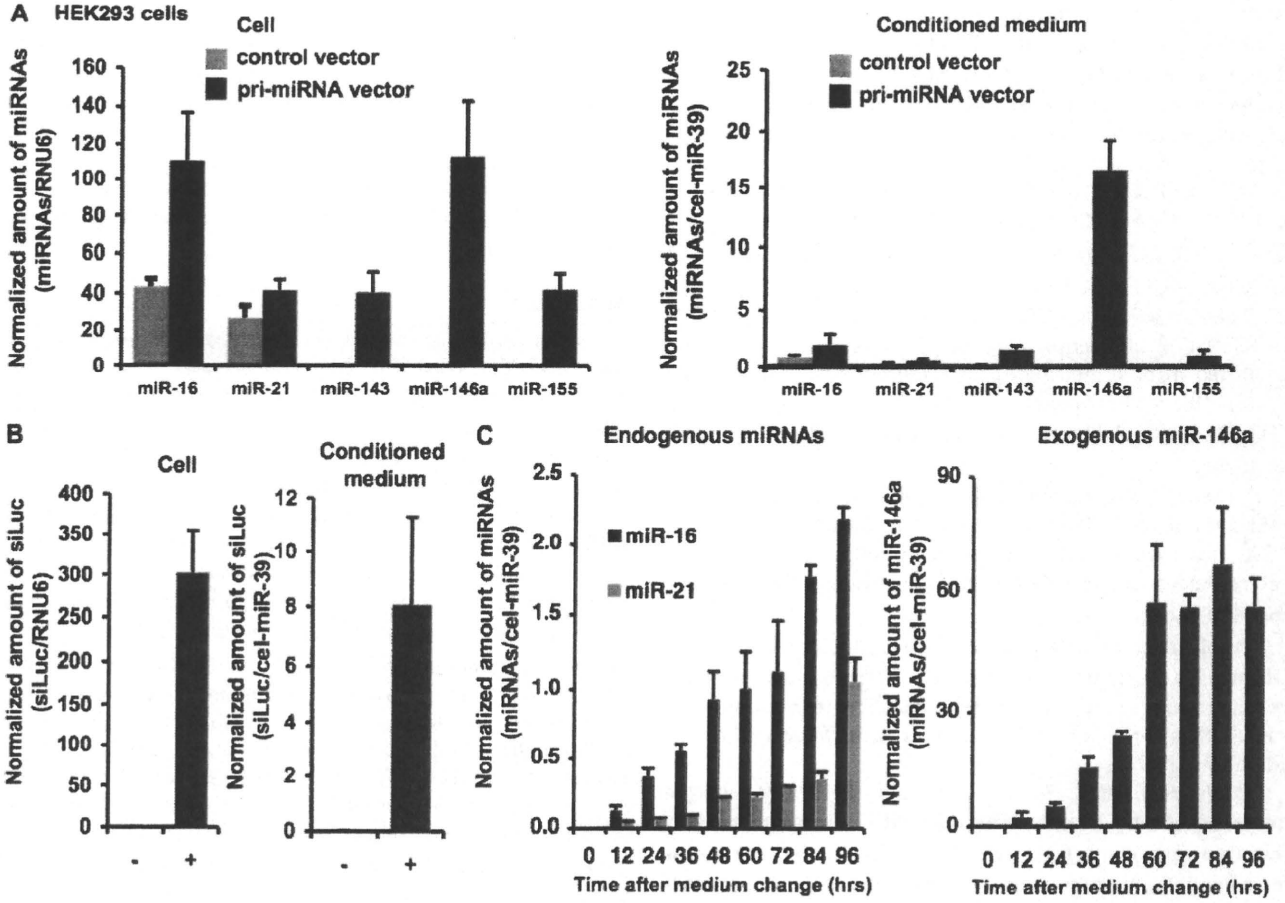

FIGURE 1. **Characterization of extracellular microRNAs.** *A*, miRNAs were released in proportion to the cellular expression level. HEK293 cells were set up at a density of 2.5×10^5 cells/well in a 24-well plate. The following day, the cells were transfected with 0.5 μg of the indicated primary miRNA expression vectors or pCMV empty vector as a control as described under "Experimental Procedures." Twenty-four h later, after washing three times by Advanced RPMI containing antibiotic-antimycotic and 2 mM L-glutamine (medium A), culture medium was switched to medium A. After a 24-h incubation, preparation of conditioned medium and isolation of total RNAs were performed as described under "Experimental Procedures." Expression levels of miRNAs were analyzed using quantitative real-time PCP (QRT-PCR). *B*, siRNAs targeting luciferase gene (*siLuc*) were secreted into culture medium. HEK293 cells were set up at a density of 2.5×10^5 cells/well in a 24-well plate. Transfection with psiRNA-LucGL3 vector (+) or control vector (−) and preparation of conditioned medium were conducted as described above. The amount of luciferase siRNAs generated from the expression vector was measured by QRT-PCR with a custom-designed TaqMan small RNA Assay (Applied Biosystems) specific for the luciferase siRNAs. *C*, time course analysis of extracellular miRNAs. Conditioned medium was collected at the indicated time and applied to quantitative miRNA RT-PCR. *A–C*, cel-miR-39 and hRNU6 were used as invariant control for conditioned medium and cell, respectively. Each *bar* is presented as mean S.E. ($n = 3$).

trifugation method. Consistent with the previous investigations, these exosome fractions were positive for a surface marker of exosome, CD63 (Fig. 2*A*). To characterize the exosomal RNAs, we conducted an electrophoresis of total RNA extracted from conditioned medium, exosomes, and their donor cells. Conditioned medium and exosomes applied to this analysis were prepared from the supernatant of the same numbers of donor cells. The Bioanalyzer 2100 profiles shown in Fig. 2*B* revealed that conditioned medium and exosome fractions share a very similar size-distribution pattern and expression intensity, which shows the enrichment of small sized RNAs, whereas the cellular RNA profile indicates two conspicuous peaks of 18 S and 28 S ribosomal RNAs and a broad peak of small RNAs. These data suggest that small RNAs are preferentially released from the cells and that most of the secreted RNAs are contained in exosome fractions. To evaluate whether extracellular miRNAs are contained inside exosomes, the conditioned medium from HEK293 cells was exposed to RNases before RNA extraction. As a result, endogenous miR-21 still existed even after 30 min of treatment with RNase A and T1 (Fig. 2*C*). Contrarily, exogenously added synthetic cel-miR-39 was completely decomposed by the same treatment (supplemental Fig. 2). Moreover, immunoprecipitant obtained with an anti-CD63 antibody was enriched in endogenous miR-16 and -155 as well as overexpressed luciferase siRNA (Fig. 2, *D* and *E*). These results collectively indicate that extracellular miRNAs are contained within the CD63-positive exosomes and therefore are protected from external RNases by the surrounding membrane.

The Secretion of miRNAs Is Regulated by a Ceramide-dependent Pathway—Exosomes are produced in MVB and released from a variety of cells. They are originally thought to function to dispose of cellular garbage, including degraded protein, but now they draw much attention as a cell-cell communication tool (5). The biogenesis of exosomes has appeared to associate with the endosomal sorting complex required for transport

Supplemental Material can be found at:
http://www.jbc.org/content/suppl/2010/03/30/M110.107821.DC1.html
http://www.jbc.org/content/suppl/2010/05/28/285.23.17442.DC1.html

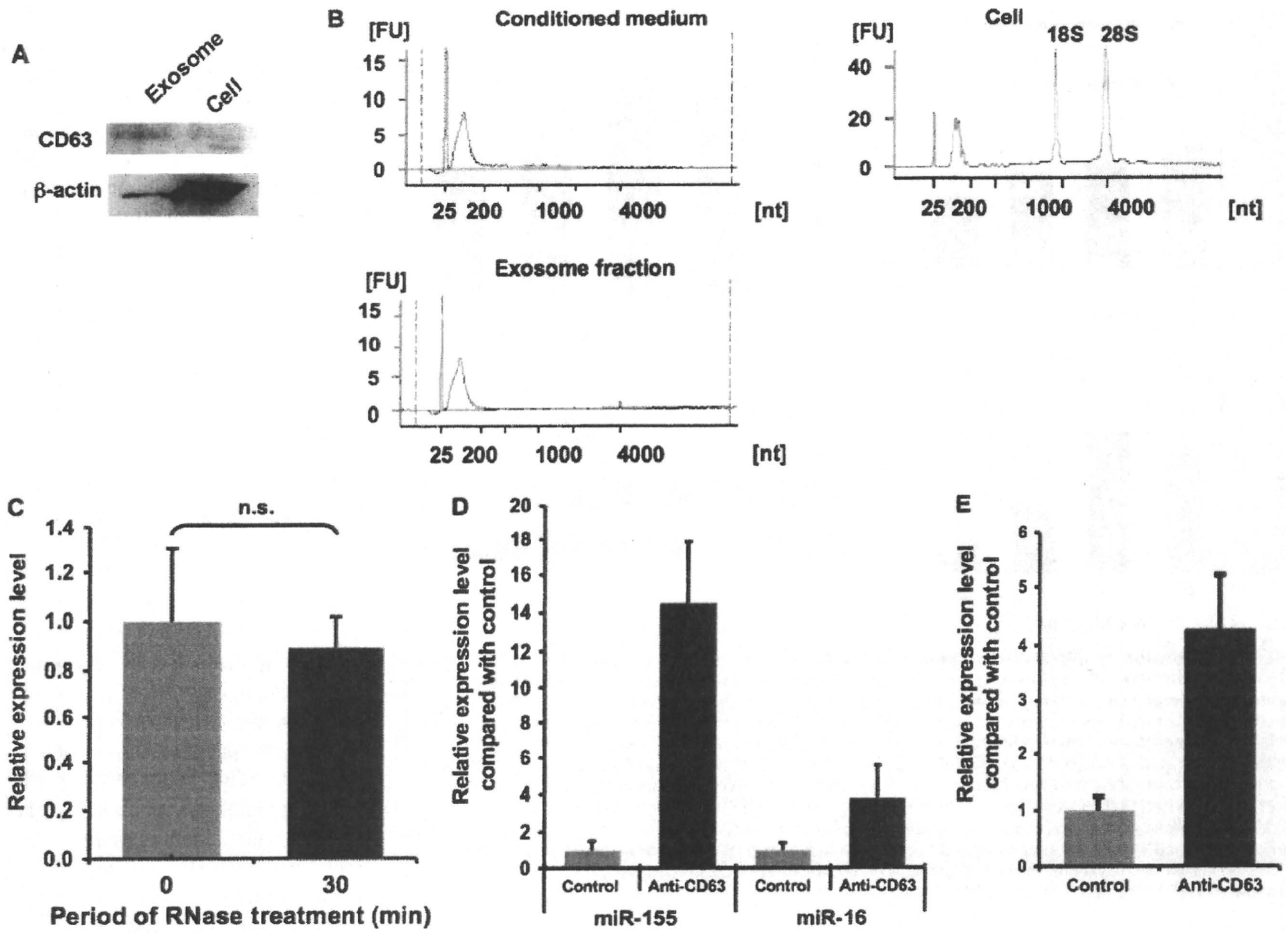

FIGURE 2. **Purification and characterization of secretory exosomes.** *A*, purified exosomes secreted from HEK293 cells are enriched in CD63 protein. The exosome fractions and whole cell lysate were analyzed by immunoblotting with an anti-CD63 antibody or anti-β-actin antibody. *B*, total RNAs isolated from conditioned medium, exosome fractions, and their donor HEK293 cells were detected using a Bioanalyzer 2100. The obtained data show the amount and the size distribution of total RNAs. The peak migrating around 25 nucleotides (*nt*) represents an internal standard. *FU*, fluorescence units. *C*, effect of RNase treatment on extracellular miR-21. Conditioned medium from HEK293 cells was exposed to RNase A and RNase T1 at 37 °C followed by the isolation of miRNAs at the indicated times. The amount of miR-21 was determined using quantitative miRNA RT-PCR. The values on the *y* axis are depicted relative to the amount of miR-21 at 0 min, which is arbitrarily defined as 1. *D* and *E*, $CD63^+$ exosome fraction is enriched in miR-155 and miR-16 (*D*) and luciferase siRNA (*E*). Conditioned medium of HEK293 cells was immunoprecipitated with anti-CD63 antibody or isotype control. The values on the *y* axis are depicted relative to control, which is arbitrarily defined as 1. *C–E*, each *bar* is presented as mean S.E. ($n = 3$). *n.s.* represents not significant.

(ESCRT) machinery because the machinery is highly involved in the exocytosis of some cellular contents and various viruses. On the other hand, Trajkovic *et al.* (18) reported that exosomes are released independently from ESCRT machinery but triggered by sphingolipid ceramide. Thus, it is still unclear whether many types of exosomal contents, such as proteins, lipids, and nucleic acids, are released by the same mechanism. To address the question as to whether miRNA secretion is regulated by the ceramide-dependent pathway or the ESCRT pathway, we first treated HEK293 cells with an nSMase inhibitor, GW4869, which is known to inhibit ceramide biosynthesis (18). As a result of this treatment, extracellular endogenous miR-16 and exogenous miR-146a were dose-dependently reduced, whereas their cellular expression levels remained unchanged (Fig. 3*A*; supplemental Fig. 3). Consistently, exosomal protein was also decreased by the treatment of GW4869 in a dose-dependent manner (Fig. 3*B*). Furthermore, a reduction in the signals of an exosome marker, CD63, was observed by immunoblotting of exosomes purified from the supernatant of the same number of GW4869-treated HEK293 cells when compared with control cells (Fig. 3*C*, *upper panel*). Nevertheless, the amounts of CD63 protein were unchanged in exosomes from GW4869-treated cells when the same amounts of exosomal proteins were analyzed (Fig. 3*C*, *lower panel*). These data show that the treatment of GW4869 reduces the amount of exosomes released into the conditioned medium but does not modify exosomal protein composition.

We next employed an RNA interference approach to knock down the expression of endogenous nSMase2 in HEK293 cells. A transfection of an siRNA duplex targeting human nSMase2 mRNAs resulted in a robust reduction of nSMase2 protein levels in HEK293 cells (Fig. 4*A*). Under these conditions, secretion of endogenous miR-16 as well as exogenous miR-146a was attenuated by the nSMase2 siRNA as compared with control cells where negative control siRNAs were transfected, whereas cellular expression of miRNAs was not changed (Fig. 4*B*). Fur-

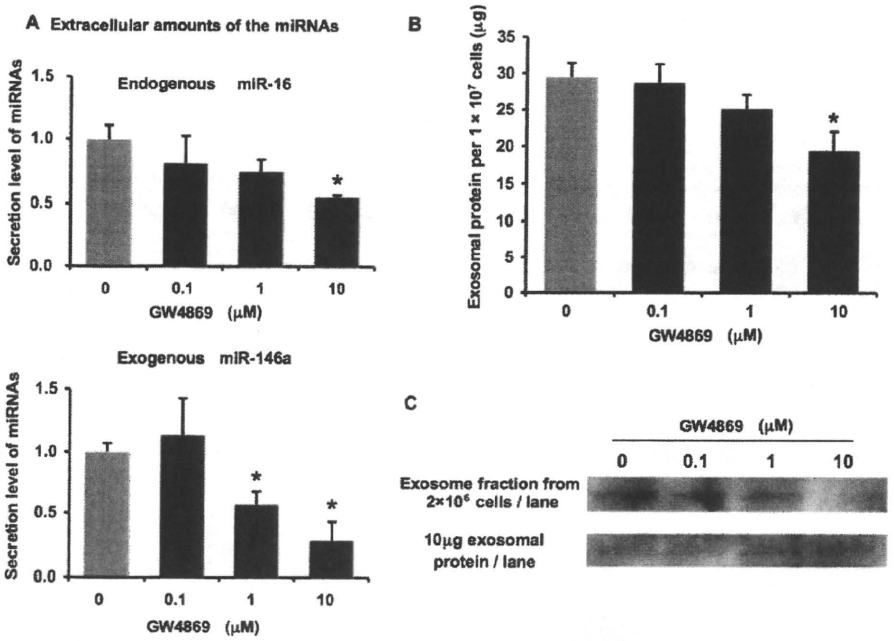

FIGURE 3. **Secretion of miRNA was attenuated by GW4869.** *A*, secretion of miRNAs was suppressed by the treatment with GW4869. HEK293 cells were transfected with pri-miR-146a vector in a 6-well plate. The cells were reseeded and cultured in a 24-well plate for 48 h in the indicated concentrations of GW4869. After the incubation, the medium was subjected to QRT-PCR for miR-16 and -146a. The values on the *y* axis are depicted relative to the amount of each miRNA at 0 μM GW4869, which is arbitrarily defined as 1. *B*, after the treatment with the indicated concentrations of GW4869 for 24 h, the total amounts of proteins in the exosomal pellet purified from large scale cultures of stably miR-146a-transduced HEK293 cells were quantified by a BCA assay and are presented as the values per 10 million secreting cells. *A* and *B*, each *bar* is presented as mean S.E. ($n = 3$). *C*, purified exosomes secreted by equal numbers of control or GW4869-treated HEK293 cells and equal amounts of total exosomal proteins (quantified by BCA assay) secreted by either control or GW4869-treated HEK293 cells were analyzed by immunoblotting for the presence of CD63 protein. (*, $p < 0.05$, **, $p < 0.005$, as compared with untreated cells; Student's *t* test).

thermore, to complement the results of this knockdown study, we observed that overexpressed human nSMase2 induced the secretion of endogenous miR-16 as well as exogenous miR-146a and luciferase siRNA from HEK293 cells without affecting cellular amounts of the miRNAs (Fig. 4, *C* and *D*, and supplemental Fig. 4*A*). Although it was already known that nSMase2 overexpression increases the amount of ceramide in the raft fraction and subsequently induces an apoptotic cell death (19), we did not observe any elevated caspase-3/7 activities in nSMase2-overexpressing cells (supplemental Fig. 4*B*). These results suggest that a ceramide-dependent secretory pathway is involved in miRNA secretion.

The Secretion of miRNAs Does Not Require ESCRT System—Gibbings *et al.* (17) showed that a knockdown of some ESCRT-associated proteins, including Alix, vps36, and hrs, deteriorated ESCRT function, resulting in an inhibition of the activity of cellular miRNAs. To examine whether Alix is involved in the secretory process of miRNAs, the knockdown experiment was performed in HEK293 cells carrying a sensor vector. As shown in Fig. 5*B*, *upper schematic*, our sensor vector is available for assessing miR-146a specific activity, which expresses firefly luciferase and *Renilla* luciferase containing complementary miR-146a sequences at its 3′-untranslated region, allowing us to simultaneously monitor transfection efficiency and miR-146a activity. Consistent with the previous finding, the depletion of Alix by an siRNA transfection fully restored the miR-146a-suppressed *Renilla* luciferase activity (Fig. 5, *A* and *B*; compare *lanes 1*, *2*, and *4*). In other words, ESCRT integrity was compromised by the Alix knockdown. On the contrary, nSMase2 siRNA had no effect on the gene silencing by miR-146a, suggesting that ceramide synthesis is irrelevant to ESCRT function (Fig. 5*B*; compare *lanes 1* and *3*). The result in the setting of non-transfection of miR-146a ruled out the possibility that the application of these siRNAs changed the basal *Renilla* luciferase activities (Fig. 5*B*; compare *lanes 4*, *5*, and *6*). QRT-PCR analysis showed that the blocked RNA silencing by the Alix knockdown was not because of the decreased amount of cellular miR-146a (Fig. 5*C*). Intriguingly, in the HEK293 cells where the ESCRT system was impaired by the Alix siRNA, we did not detect any significant difference of the amount of extracellular miR-146a as compared with a control transfectant (Fig. 5*D*). Taken together with the results of Figs. 3 and 4, it is unequivocally demonstrated that secretion of miRNAs depends on a ceramide-triggered secretory mechanism but not ESCRT machinery.

Secretory Small RNAs Can Be Transferred to Recipient Cells—Our finding that miRNA secretion is tightly regulated by ceramide biosynthesis inspires us to envisage that extracellular miRNAs are not just discards from the originating cells but biologically active molecules. In fact, many reports suggest that small RNAs migrate beyond their cell origin and function in the recipient cells (6, 9). To test whether or not artificial small RNA can be transported into recipient cells under our experimental conditions, we treated firefly luciferase stably expressing HEK293 cells with a conditioned medium enriched in the luciferase siRNAs. The amounts of small RNAs in the conditioned medium were evaluated by QRT-PCR as described under "Experimental Procedures." As a result, the luciferase activities were negatively regulated by the treatment of conditioned medium containing 200 pM luciferase siRNAs as compared with control conditioned medium and fresh RPMI medium as well as miR-146a-enriched conditioned medium (Fig. 6*A*). In addition to artificial siRNAs, we next examined a transfer of a class of naturally occurring small RNAs, miRNAs. To measure a direct regulation of gene expression by extracellular miRNAs, we performed a reporter assay based on the sensor vector according to an experimental scheme illustrated in Fig. 6*B*. As shown in Fig. 6*C*, the normalized *Renilla* luciferase activities were dose-dependently reduced by the treatment of miR-146a-enriched conditioned medium derived from COS-7 and HEK293 cells transfected with pri-miR-146a expression vec-

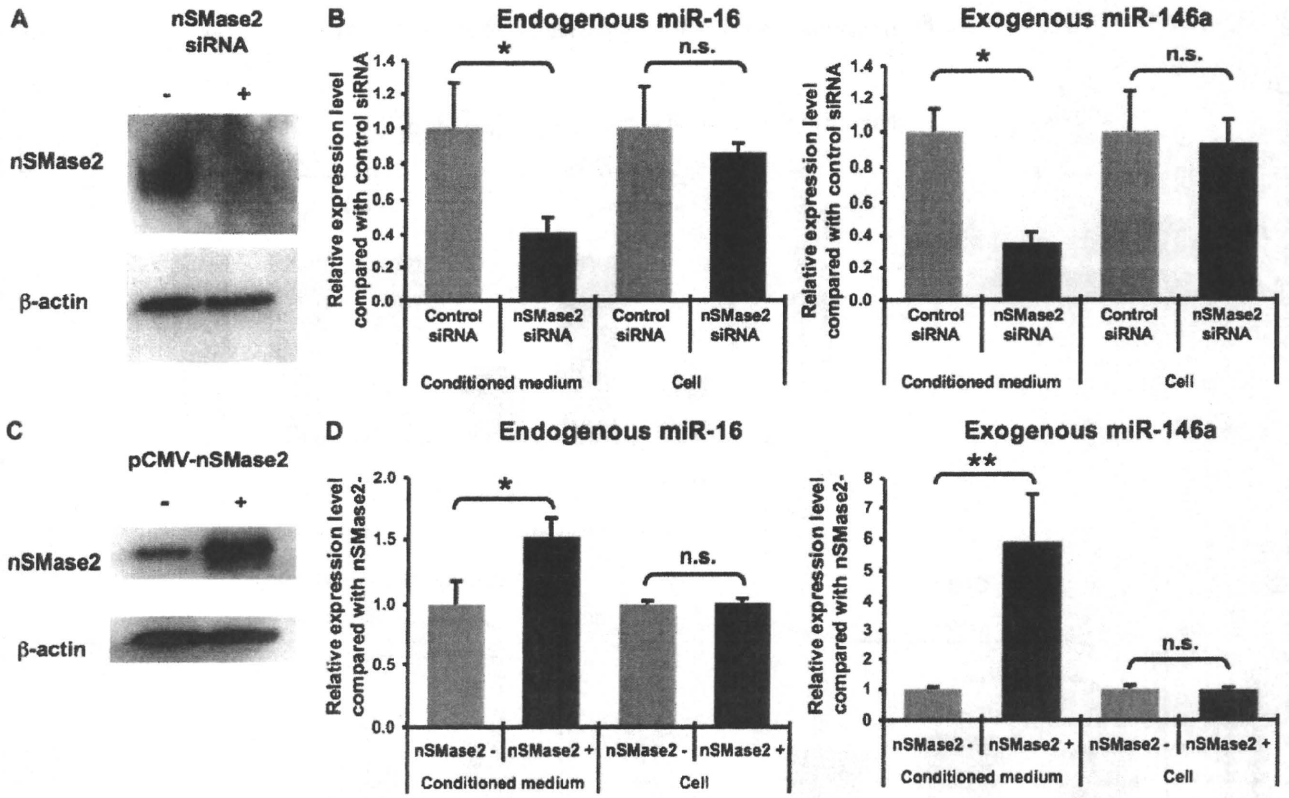

FIGURE 4. **miRNAs were secreted through nSMase2-dependent pathway.** *A* and *B*, siRNA-mediated knockdown of nSMase2. HEK293 cells were transfected with pri-miR-146a vector in a 6-well plate. One day later, these cells were reseeded in a 24-well plate and transfected with either negative control or nSMase2 siRNA. The following day, conditioned medium and cell extract were applied to QRT-PCR for miR-16 as well as miR-146a (*B*). In parallel, cell extract was applied to immunoblot for nSMase2 and β-actin proteins (*A*). The values on the *y* axis are depicted relative to the amount of miRNAs of control, which is arbitrarily defined as 1. *C* and *D*, augmentation of miRNA secretion by overexpressed human nSMase2. HEK293 cells were transfected with human nSMase2 expression vector or control vector, along with pri-miR-146a vector. After a 24-h incubation, conditioned medium and cell extract were applied to QRT-PCR (*D*), and cell extract was applied to immunoblot (*C*). The values on the *y* axis are depicted relative to the amount of miRNAs of nSMase2−, which is arbitrarily defined as 1. *B* and *D*, each *bar* is presented as mean S.E. ($n = 3$). (*, $p < 0.05$, **, $p < 0.005$, as compared with control cells; Student's *t* test); *n.s.* represents not significant.

tors. This effect was not due to a transfer of free miRNAs remaining in cellular debris and conditioned medium because a direct addition of 100 nM naked miR-146a analogues did not change the luciferase activity (supplemental Fig. 5). Furthermore, to exclude the possibility that the inhibitory effect is independent of the specific interaction between the transferred miR-146a and the complementary binding sites in the sensor vector, we used a mutated miR-146a sensor vector constructed as described under "Experimental Procedures." As shown in Fig. 6*D*, the normalized *Renilla* luciferase activities from the mutated sensor vector were not changed by the addition of the conditioned medium from miR-146a-overexpressing HEK293 cells. These results show that extracellular miRNAs packaged in secretory exosome vesicles can be delivered into recipient cells and act as physiologically functional molecules to exert gene silencing through the same mechanism as cellular miRNAs.

Secretory Tumor-suppressive miRNAs Attenuate PC-3M Cell Proliferation—To gain further insight into the biological activity of secretory miRNAs, we investigated whether they can make an impact on a cellular phenotype. miR-146a is known to be down-regulated in prostate cancer (20), and reconstitution of its expression results in growth inhibition of prostate cancer cells (21). As schematically depicted in Fig. 7*A*, supernatants containing transduced miR-146a derived from COS-7 cells were added to the culture medium of metastatic prostate cancer cell line PC-3M-luc cells. This cell line stably harbors a firefly luciferase gene, enabling us to assess cell numbers with the luciferase activity. After a 3-day incubation, PC-3M-luc cells showed an ~20% decrease in proliferation in the presence of 21 pM miR-146a in the conditioned medium, whereas liposomally transfected synthetic miRNAs at 10 pM suppressed cell growth to a similar extent (Fig. 7*B*). To determine whether extracellular miRNA exerts regulatory action on its target gene, we examined the expression of ROCK1, a target gene for miR-146a, in the treatment with extracellular miR-146a (21). The addition of the conditioned medium of miR-146a-transduced COS-7 cells significantly knocked down ROCK1 protein expression in PC-3M-luc cells to the same degree as the miR-146a analogue molecule under conditions where the amount of β-actin was not affected (Fig. 7*C*). To confirm that the cell growth inhibition resulted from the transferred exosomal miR-146a, we examined whether the suppressive effect can be cancelled by a reduced exosome secretion. Conditioned medium from GW4869-treated donor cells had no inhibitory activity on cell proliferation after a 4-day incubation (Fig. 7*D*; compare *lanes 1* and *2*). We also did not observe any direct effect of GW4869 on the restoration of miR-146a-suppressed cell

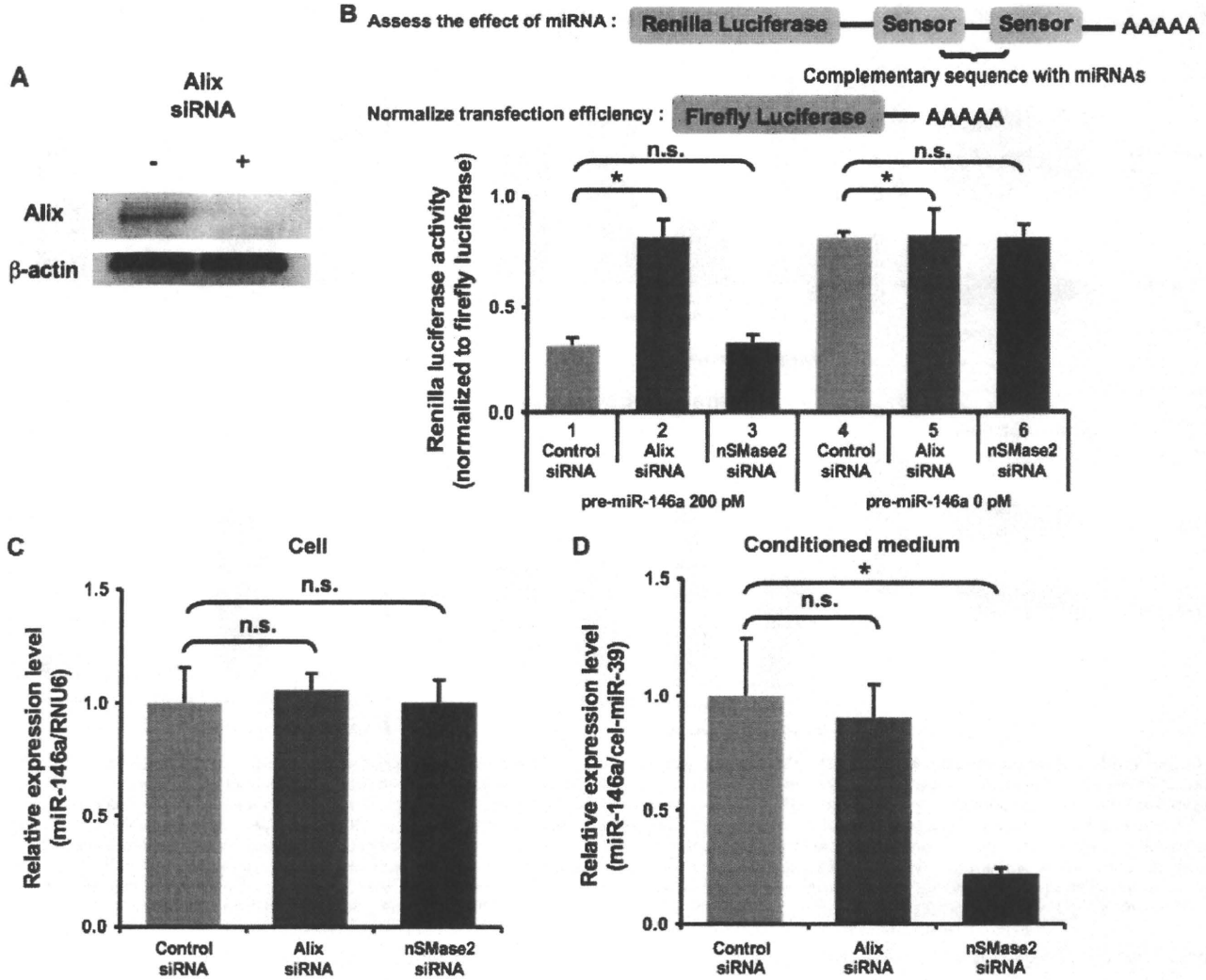

FIGURE 5. **The secretion of miRNAs does not require ESCRT system.** *A*, knockdown of human Alix protein. HEK293 cells transfected with negative control siRNA or Alix siRNA were harvested and applied to immunoblot for Alix and β-actin proteins. *B*, the depletion of Alix impaired miRNA activity. *Upper schematic*, our sensor vector possesses *Renilla* luciferase and firefly luciferase for assessing the miRNA activity and for normalizing transfection efficiency, respectively. Lower *graph*, HEK293 cells were transfected with 0.1 μg of miR-146a sensor vector and the indicated siRNAs together with 200 or 0 pM pre-miR-146a in a 96-well plate. The following day, the cells were applied to a Dual luciferase reporter assay. The values on the *y* axis are normalized *Renilla* luciferase activity. *C* and *D*, cellular and extracellular miR-146a were not affected by Alix siRNA. MiR-146a stably overexpressing HEK293 cells were transfected with the indicated siRNAs. After the medium switch, the cells were cultured for another 24 h, and the cell lysate (*C*) and conditioned medium (*D*) were then applied to miRNA QRT-PCR analysis. The values on the *y* axis are depicted relative to control siRNA, which is arbitrarily defined as 1. *B–D*, each *bar* is presented as mean S.E. ($n = 3$). (*, $p < 0.05$, **, $p < 0.005$, as compared with control siRNAs; Student's *t* test); *n.s.* represents not significant.

growth (Fig. 7*D*; compare *lanes 3* and *4*). These findings suggest that itinerant exosomal miRNAs can induce some phenotypic changes in the recipient cells.

DISCUSSION

Our data provide a fresh insight into the secretory machinery of miRNAs. Through our mechanistic studies with a chemical inhibitor as well as nSMase2 overexpression and knockdown, we contend that miRNAs can be incorporated into exosomes and released via a ceramide-dependent pathway independently of ESCRT machinery. It remains elusive, however, how miRNAs are sorted into exosomes for their secretion. Two recent studies provide evidences that ESCRT complex associates with components of miRNA effector complexes and that RNA silencing takes place on MVB (22). Taken together, MVB could be a crossroads of miRNAs bound for the secretory pathway and gene-silencing cycle. Further investigations are needed to unveil a sorting mechanism by which miRNAs are determined to be secreted or to stay and function in their originating cells.

There is growing evidence that secretory miRNAs play a role in a variety of physiological phenomena. Zernecke *et al.* (9) showed that the transfer of miR-126 loaded into endothelial apoptotic bodies induced the expression of CXCL12 and the recruitment of progenitor cells, thereby alleviating atherosclerosis. Additionally, Rechavi *et al.* (8) proposed that viruses could tamper with the host immune response by transportation of viral non-autonomously encoded small RNAs. Both vascular protection and manipulation of the immune system by viruses occur for a long term. These find-

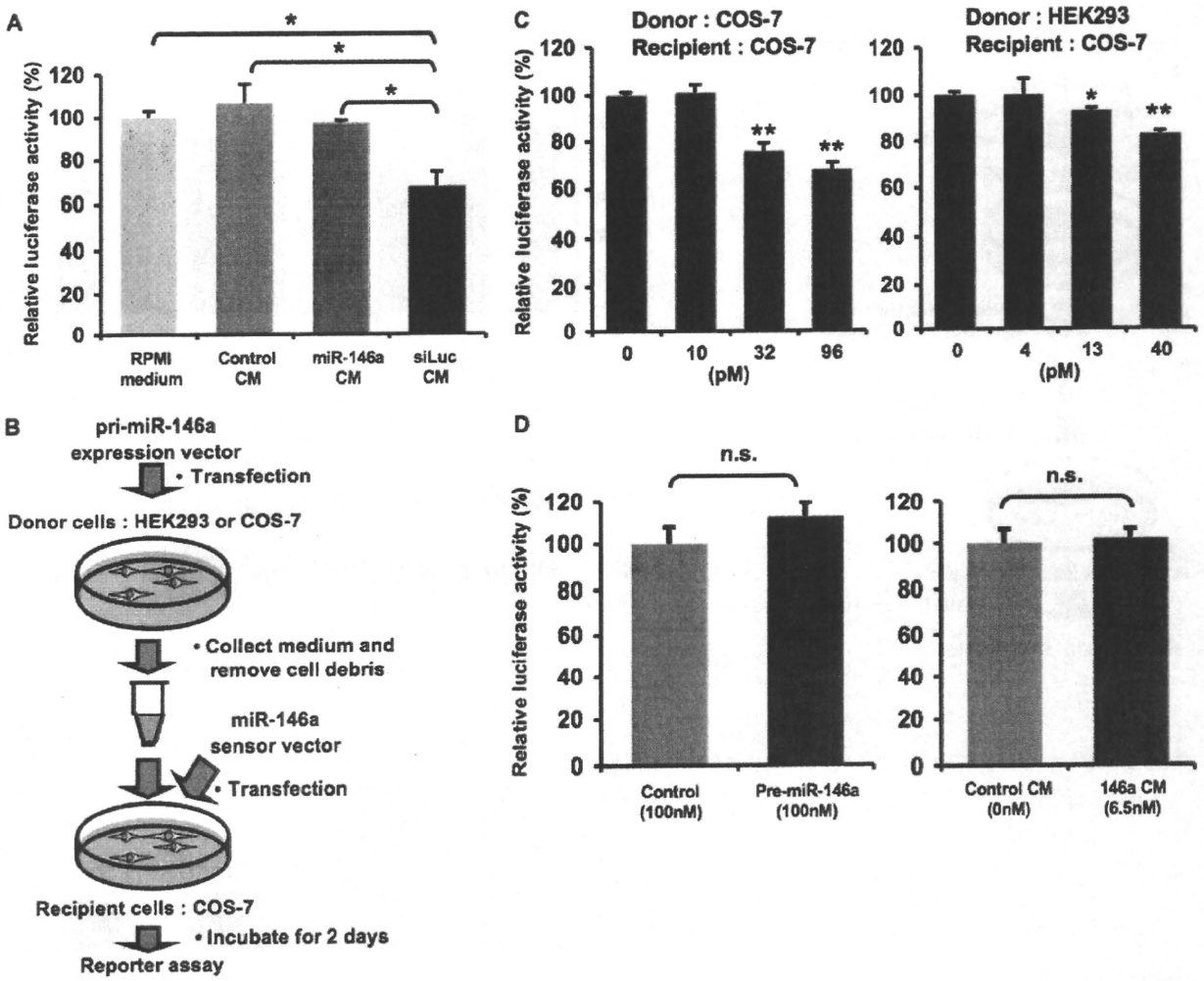

FIGURE 6. **Secretory small RNAs can be transferred to recipient cells.** *A*, treatment with conditioned medium enriched in luciferase siRNA down-regulated luciferase activity. HEK293 cells stably transduced with firefly luciferase were incubated with the indicated medium for 3 days. The conditioned medium was prepared from HEK293 cells transfected with psiRNA-LucGL3 or empty vector. The luciferase siRNA was not detected in RPMI medium and control CM as well as miR-146a CM using QRT-PCR, whereas luciferase siRNA (*siLuc*) CM contained 200 pM luciferase siRNA as calculated under "Experimental Procedures." The concentration of miR-146a in miR-146a CM was 123 pM. The cells were harvested and applied to luciferase reporter assay. The values on the *y* axis are depicted relative to firefly luciferase activity of RPMI medium-treated cells, which is defined as 100%. *B*, the diagram shows a reporter assay for testing the direct regulation of target gene expression by extracellular miRNAs. *C*, extracellular miR-146a derived from COS-7 and HEK293 cells suppressed luciferase activity of the sensor vector. COS-7 cells transfected with miR-146a sensor vector were used as recipient cells. The recipient cells were incubated in the conditioned medium containing extracellular miRNAs of the indicated concentrations. After a 2-day incubation, luciferase reporter assay was performed as described under "Experimental Procedures." *D*, miR-146a did not reduce luciferase activity from the mutated sensor vector. COS-7 cells transfected with the mutated miR-146a sensor vector were used as recipient cells. The recipient cells were transfected with synthetic miRNAs (*left graph*) or incubated in the conditioned medium containing extracellular miRNAs at the indicated concentrations (*right graph*). Luciferase assay was carried out as described above. *C* and *D*, the values on the *y* axis are depicted relative to normalized *Renilla* luciferase activity of control cells, which is defined as 100%. *A*, *C*, and *D*, each *bar* is presented as mean S.E. ($n = 3$). (*, $p < 0.05$, **, $p < 0.005$, as compared with control recipient cells; Student's *t* test); *n.s.* represents not significant.

ings prompt us to conceive of the idea that secretory miRNAs could mainly serve in chronic biological events, such as the formation of a tumor microenvironment.

Many tumors have a remarkable ability to mold their stromal environment to their own advantage (23, 24). Recent studies show the importance of communication between cancer cells and their surroundings through shedding of membrane exosomes, which can fuse to cells in the vicinity (7, 25, 26). For instance, epidermal growth factor receptor vIII proteins were transferred into glioma cells lacking epidermal growth factor receptor vIII via secretory membrane microvesicles (26). Together, membrane microvesicles or exosomes of cancer cells can contribute to a horizontal propagation of oncogenes and their associated transforming phenotype among subsets of cancer cells. Here, we show that re-expression of miR-146a through intercellular transfer leads to cell growth inhibition of PC-3M cells, where the expression of the miRNA is at a very low level. It is well known that many kinds of miRNAs are down-regulated in cancer cells, resulting in tumorigenesis, tumor progression, and metastasis (27). We therefore hypothesize that down-regulated miRNAs in cancer cells are compensated during the initial stage of tumorigenesis by the surrounding cells that supply exosomes containing the decreased miRNAs. However, once the surrounding cells cannot meet the demand, cancer cells end up entering an advanced stage.

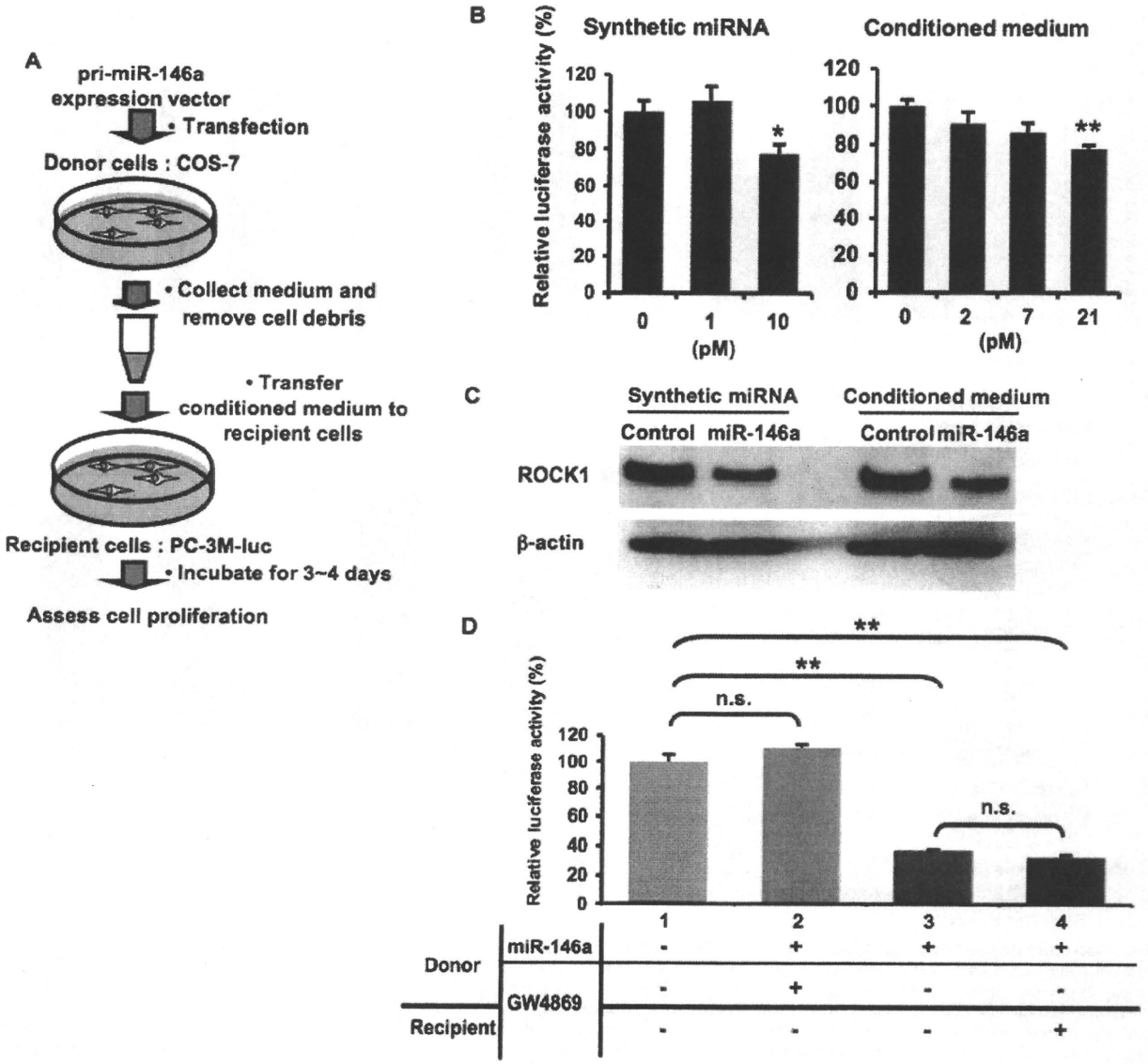

FIGURE 7. **Secretory tumor-suppressive miRNAs attenuated PC-3M cell proliferation.** *A*, schematic representation of a cell proliferation assay. *B*, cell growth inhibition by synthetic miR-146a and extracellular miR-146a. PC-3M-luc cells were transfected with synthetic miRNAs (*left graph*) or incubated in the conditioned medium containing extracellular miRNAs at the indicated concentrations (*right graph*) followed by cell growth assay as described under "Experimental Procedures." *C*, miR-146a-mediated ROCK1 suppression in PC-3M-luc cells. The final concentrations of synthetic and extracellular miR-146a are 10 and 21 pM, respectively. *D*, the treatment with GW4869 to donor cells restored the reduced cell growth by the exosomal miR-146a. Donor COS-7 cells transfected with pri-miR-146a expression vector were incubated in the presence (*lane 2*) or absence of 10 μM GW4869 for 3 days. The conditioned medium from COS-7 cells transfected with empty vector was used as a control (*lane 1*). GW4869-untreated conditioned medium enriched in miR-146a was divided into two aliquots, one of which was treated with 10 μM GW4869 (*lane 3*) and the other of which was not treated (*lane 4*) before the transfer to recipient cells. The following assay was conducted as described above. *B* and *D*, the values on the *y* axis are depicted relative to normalized *Renilla* luciferase activity of control cells, which is defined as 100%. Each *bar* is presented as mean S.E. ($n = 3$). (*, $p < 0.05$, **, $p < 0.005$, as compared with untreated PC-3M-luc cells; Student's *t* test); *n.s.* represents not significant.

Secretory miRNAs could be conducive to the maintenance and surveillance system against cancer progression.

Small RNAs including antisense, siRNA, and miRNA are emerging as promising therapeutic agents against a wide array of diseases (28). Effective delivery of these molecules is crucial to their successful clinical application. Now, exosomes have entered the limelight in delivery of therapeutic nucleic acids with their ability to transfer exogenous miRNAs into tumor cells. Exosomes are naturally produced membrane vesicles that circulate in the bloodstream and are taken up by various types of cells. These aspects might be beneficial for the improvement of durability, stability, and safety for *in vivo* delivery. In fact, tumor exosomes generated tumor regression *in vivo*, acting as a cancer vaccine through their capacity of antigen presentation (29). It is essential to examine whether exosomes can deliver their cargoes in an *in vivo* animal model.

In conclusion, we revealed the secretory machinery of miRNAs and their intercellular transfer. Our results raise the possibility that in the animal kingdom, circulating miRNAs

could play a pivotal and general role as a signaling molecule in physiological and pathological events. We anticipate that our study could pave the way for explorations of signal network mediated by secretory miRNAs.

Acknowledgment—We thank Ayano Matsumoto for excellent technical assistance.

REFERENCES

1. Fleischhacker, M., and Schmidt, B. (2007) *Biochim. Biophys. Acta* **1775,** 181–232
2. El-Hefnawy, T., Raja, S., Kelly, L., Bigbee, W. L., Kirkwood, J. M., Luketich, J. D., and Godfrey, T. E. (2004) *Clin. Chem.* **50,** 564–573
3. Tsui, N. B., Ng, E. K., and Lo, Y. M. (2002) *Clin. Chem.* **48,** 1647–1653
4. Hasselmann, D. O., Rappl, G., Tilgen, W., and Reinhold, U. (2001) *Clin. Chem.* **47,** 1488–1489
5. Cocucci, E., Racchetti, G., and Meldolesi, J. (2009) *Trends Cell Biol.* **19,** 43–51
6. Valadi, H., Ekström, K., Bossios, A., Sjöstrand, M., Lee, J. J., and Lötvall, J. O. (2007) *Nat. Cell Biol.* **9,** 654–659
7. Skog, J., Würdinger, T., van Rijn, S., Meijer, D. H., Gainche, L., Sena-Esteves, M., Curry, W. T., Jr., Carter, B. S., Krichevsky, A. M., and Breakefield, X. O. (2008) *Nat. Cell Biol.* **10,** 1470–1476
8. Rechavi, O., Erlich, Y., Amram, H., Flomenblit, L., Karginov, F. V., Goldstein, I., Hannon, G. J., and Kloog, Y. (2009) *Genes Dev.* **23,** 1971–1979
9. Zernecke, A., Bidzhekov, K., Noels, H., Shagdarsuren, E., Gan, L., Denecke, B., Hristov, M., Köppel, T., Jahantigh, M. N., Lutgens, E., Wang, S., Olson, E. N., Schober, A., and Weber, C. (2009) *Sci. Signal.* **2,** ra81
10. Kim, V. N., Han, J., and Siomi, M. C. (2009) *Nat. Rev. Mol. Cell Biol.* **10,** 126–139
11. Croce, C. M. (2009) *Nat. Rev. Genet.* **10,** 704–714
12. Lawrie, C. H., Gal, S., Dunlop, H. M., Pushkaran, B., Liggins, A. P., Pulford, K., Banham, A. H., Pezzella, F., Boultwood, J., Wainscoat, J. S., Hatton, C. S., and Harris, A. L. (2008) *Br. J. Haematol.* **141,** 672–675
13. Mitchell, P. S., Parkin, R. K., Kroh, E. M., Fritz, B. R., Wyman, S. K., Pogosova-Agadjanyan, E. L., Peterson, A., Noteboom, J., O'Briant, K. C., Allen, A., Lin, D. W., Urban, N., Drescher, C. W., Knudsen, B. S., Stirewalt, D. L., Gentleman, R., Vessella, R. L., Nelson, P. S., Martin, D. B., and Tewari, M. (2008) *Proc. Natl. Acad. Sci. U.S.A.* **105,** 10513–10518
14. Chen, X., Ba, Y., Ma, L., Cai, X., Yin, Y., Wang, K., Guo, J., Zhang, Y., Chen, J., Guo, X., Li, Q., Li, X., Wang, W., Zhang, Y., Wang, J., Jiang, X., Xiang, Y., Xu, C., Zheng, P., Zhang, J., Li, R., Zhang, H., Shang, X., Gong, T., Ning, G., Wang, J., Zen, K., Zhang, J., and Zhang, C. Y. (2008) *Cell Res.* **18,** 997–1006
15. Taylor, D. D., and Gercel-Taylor, C. (2008) *Gynecol. Oncol.* **110,** 13–21
16. Takeshita, F., Patrawala, L., Osaki, M., Takahashi, R. U., Yamamoto, Y., Kosaka, N., Kawamata, M., Kelnar, K., Bader, A. G., Brown, D., and Ochiya, T. (2010) *Mol. Ther.* **18,** 181–187
17. Gibbings, D. J., Ciaudo, C., Erhardt, M., and Voinnet, O. (2009) *Nat. Cell Biol.* **11,** 1143–1149
18. Trajkovic, K., Hsu, C., Chiantia, S., Rajendran, L., Wenzel, D., Wieland, F., Schwille, P., Brügger, B., and Simons, M. (2008) *Science* **319,** 1244–1247
19. Hannun, Y. A., and Obeid, L. M. (2002) *J. Biol. Chem.* **277,** 25847–25850
20. Volinia, S., Calin, G. A., Liu, C. G., Ambs, S., Cimmino, A., Petrocca, F., Visone, R., Iorio, M., Roldo, C., Ferracin, M., Prueitt, R. L., Yanaihara, N., Lanza, G., Scarpa, A., Vecchione, A., Negrini, M., Harris, C. C., and Croce, C. M. (2006) *Proc. Natl. Acad. Sci. U.S.A.* **103,** 2257–2261
21. Lin, S. L., Chiang, A., Chang, D., and Ying, S. Y. (2008) *RNA* **14,** 417–424
22. Lee, Y. S., Pressman, S., Andress, A. P., Kim, K., White, J. L., Cassidy, J. J., Li, X., Lubell, K., Lim do, H., Cho, I. S., Nakahara, K., Preall, J. B., Bellare, P., Sontheimer, E. J., and Carthew, R. W. (2009) *Nat. Cell Biol.* **11,** 1150–1156
23. Bhowmick, N. A., Neilson, E. G., and Moses, H. L. (2004) *Nature* **432,** 332–337
24. Mantovani, A., Allavena, P., Sica, A., and Balkwill, F. (2008) *Nature* **454,** 436–444
25. Wolfers, J., Lozier, A., Raposo, G., Regnault, A., Théry, C., Masurier, C., Flament, C., Pouzieux, S., Faure, F., Tursz, T., Angevin, E., Amigorena, S., and Zitvogel, L. (2001) *Nat. Med.* **7,** 297–303
26. Al-Nedawi, K., Meehan, B., Micallef, J., Lhotak, V., May, L., Guha, A., and Rak, J. (2008) *Nat. Cell Biol.* **10,** 619–624
27. Bonci, D., Coppola, V., Musumeci, M., Addario, A., Giuffrida, R., Memeo, L., D'Urso, L., Pagliuca, A., Biffoni, M., Labbaye, C., Bartucci, M., Muto, G., Peschle, C., and De Maria, R. (2008) *Nat. Med.* **14,** 1271–1277
28. Castanotto, D., and Rossi, J. J. (2009) *Nature* **457,** 426–433
29. Mignot, G., Roux, S., Thery, C., Ségura, E., and Zitvogel, L. (2006) *J. Cell Mol. Med.* **10,** 376–388

Published OnlineFirst April 13, 2010; DOI:10.1158/1078-0432.CCR-09-2214

Clinical Cancer Research

Combined Functional Genome Survey of Therapeutic Targets for Hepatocellular Carcinoma

Reiko Satow, Miki Shitashige, Yae Kanai, et al.

Clin Cancer Res 2010;16:2518-2528. Published OnlineFirst April 13, 2010.